The Greenland-Norwegian Seaway: A key area for understanding Late Jurassic to Early Cretaceous paleoenvironments

Jörg Mutterlose,[1] Hans Brumsack,[2] Sascha Flögel,[3] William Hay,[3] Christian Klein,[1] Uwe Langrock,[4] Marcus Lipinski,[2] Werner Ricken,[5] Emanuel Söding,[3] Rüdiger Stein,[4] and Oliver Swientek[5]

Received 22 January 2001; revised 24 April 2002; accepted 9 July 2002; published 26 February 2003.

[1] The paleoclimatology and paleoceanology of the Late Jurassic and Early Cretaceous are of special interest because this was a time when large amounts of marine organic matter were deposited in sediments that have subsequently become petroleum source rocks. However, because of the lack of outcrops, most studies have concentrated on low latitudes, in particular the Tethys and the "Boreal Realm," where information has been based largely on material from northwest Germany, the North Sea, and England. These areas were all south of 40°N latitude during the Late Jurassic and Early Cretaceous. We have studied sediment samples of Kimmeridgian (~154 Ma) to Barremian (~121 Ma) age from cores taken at sites offshore mid-Norway and in the Barents Sea that lay in a narrow seaway connecting the Tethys with the northern polar ocean. During the Late Jurassic-Early Cretaceous these sites had paleolatitudes of 42–67°N. The Late Jurassic-Early Cretaceous sequences at these sites reflect the global sea-level rise during the Volgian-Hauterivian and a climatic shift from warm humid conditions in Volgian times to arid cold climates in the early Hauterivian. The sediments indicate orbital control of climate, reflected in fluctuations in the clastic influx and variations in carbonate and organic matter production. Trace element concentrations in the Volgian-Berriasian sediments suggest that the central part of the Greenland-Norwegian Seaway might have had suboxic bottom water beneath an oxic water column. Both marine and terrigenous organic matter are present in the seaway sediments. The Volgian-Berriasian strata have unusually high contents of organic carbon and are the source rocks for petroleum and gas fields in the region. The accumulation of organic carbon is attributed to restricted conditions in the seaway during this time of low sea level. It might be that the Greenland-Norwegian segment was the deepest part of the transcontinental seaway, bounded at both ends by relatively shallow swells. The decline in organic matter content of the sediments in the Valanginian-Hauterivian indicates greater ventilation and more active flow through the seaway as the sea level rose. The same benthic foraminifera assemblages are encountered throughout the seaway. Endemic assemblages of arenaceous foraminifera in the Volgian-Berriasian give way to more diverse and cosmopolitan Valanginian-Hauterivian benthic communities that include calcareous species. The foraminiferal assemblages also suggest low oxygen content bottom waters during the earlier Cretaceous, changing to more fully oxygenated conditions later. The calcareous nannoplankton, particularly *Crucibiscutum salebrosum*, which is rare at low latitudes and abundant in high latitudes, reflect the meridional thermal gradient. They indicate that the Greenland-Norwegian segment of the seaway was north of a subtropical frontal zone that acted as a barrier between the Tethyan and Boreal Realms. This implies the existence of stable climatic belts during the early Valanginian and Hauterivian, significant meridional temperature gradients, and moderate "ice house" conditions. *INDEX TERMS:* 1050 Geochemistry: Marine geochemistry (4835, 4850); 3022 Marine Geology and Geophysics: Marine sediments—processes and transport; 3030 Marine Geology and Geophysics: Micropaleontology; 4267 Oceanography: General: Paleoceanography; *KEYWORDS:* Greenland-Norwegian seaway, late Jurassic, early Cretaceous, paleoceanography

Citation: Mutterlose, J., et al., The Greenland-Norwegian Seaway: A key area for understanding Late Jurassic to Early Cretaceous paleoenvironments, *Paleoceanography*, *18*(1), 1010, doi:10.1029/2001PA000625, 2003.

[1]Institut für Geologie, Mineralogie und Geophysik, Ruhr Universität Bochum, Bochum, Germany.

[2]Institut für Chemie und Biologie des Meeres, Universität Oldenburg, Oldenburg, Germany.

[3]GEOMAR, Forschungszentrum für Marine Geowissenschaften, Kiel, Germany.

[4]Alfred Wegener Institut für Polar- und Meeresforschung, Bremerhaven, Germany.

[5]Geologisches Institut, Universität Köln, Köln, Germany.

0883-8305/03/2001PA000625

Table 1. Locations, Water Depths, Stratigraphic Ages, and Type and Number of Samples Taken at Sites off Norway[a]

Site	Latitude	Longitude	Water Depth, m	Stratigraphic Age Range
6307/07-U-02	63°27′54″N	07°14′44″E	290	Kimmeridgian-Valanginian
6814/04-U-02	68°39′45″N	14°09′47″E	233	Volgian-Barremian
7430/10-U-01	74°12′47″N	30°14′44″E	335	Kimmeridgian-Barremian
7425/09-U-01	74°29′25″N	25°46′19″E	355	Berriasian-Barremian
7231/01-U-01	72°45′12″N	31°07′30″E	278	Oxfordian-Barremian

Site	ISO	IGC	OGC	CN	F
6307/07-U-02	22 *22*	71	71	68 *27*	81 *42*
6814/04-U-02	90 *84*	87	87		115 *93*
7430/10-U-01	35 *21*	26 122	26 *122*	143 *15*	26 *11*
7425/09-U-01				24 *15*	
7231/01-U-01				24 *15*	

[a]where ISO = isotopic analyses, bulk samples indicated in italics, shell samples in normal type; IGC = inorganic geochemistry; OGC = organic geochemistry, samples taken for high-resolution studies in italics; CN = calcareous nannoplankton, total samples taken in normal type, samples found to contain nannofossils in italics; F = Foraminifera, total samples taken in normal type, samples found to contain foraminifera in italics.

1. Introduction

[2] Understanding of later Mesozoic paleoclimates and paleoceanography has increased greatly in the past decade as summarized by papers by *Barrera and Johnson* [1999] and *Huber et al.* [2000]. The notion of the Jurassic and Cretaceous being a time of monotonously warm equable conditions and sluggish ocean circulation has given way to much more varied views of changing paleoclimatic and oceanographic conditions, especially during the Late Jurassic and Early Cretaceous. Global paleoenvironmental changes should be most clearly reflected in the high latitudes, but because of the paucity of outcrops and material, most studies have concentrated on low latitudes, in particular the Tethys region [*Kollmann and Zapfe*, 1992]. Information on the "Boreal Realm" [*Neumayr*, 1883] has been based largely on material from northwest Germany, the North Sea, and England [*Horna et al.*, 1998]. These areas were all south of 40°N latitude during the Late Jurassic and Early Cretaceous. In order to obtain a better understanding of the Cretaceous of the Northern Hemisphere, information already available from low-latitude Deep Sea Drilling Project (DSDP) and Ocean Drilling Project (ODP) sites, France, Italy, Romania, Poland, and northwest Europe (Germany, North Sea, and England) needed to be complemented by studies of material from higher paleolatitudes. We have studied sediment samples of Kimmeridgian (∼154 Ma) to Barremian (∼121 Ma) age from cores taken at sites on the Norwegian shelves. The sites lay at paleolatitudes of 42–67°N during the Late Jurassic-Early Cretaceous in a narrow seaway between Greenland and Norway which connected the Tethys with the northern polar ocean.

[3] The geology of these sites have been discussed by *Århus* [1991], *Leith et al.* [1992], *Smelror* [1994], *Smelror et al.* [1994, 1998, 2001a, 2001b], *Jongepier et al.* [1996], *Dypvik et al.* [1996], and *Mutterlose and Kessels* [2000].

[4] Specifically, we were seeking answers to the following questions:

1. Do the sediments reflect Milankovitch orbital cycle control of the high-latitude climate?
2. What do major and trace elements indicate concerning the paleoenvironment in the seaway?
3. What is the composition and origin of marine and terrigenous organic matter in the seaway?
4. What do calcareous nannofossils and foraminifera indicate about flow through the seaway?
5. What were the paleoclimatic and paleoceanographic conditions in the Boreal-Arctic region during earliest Cretaceous times?

2. Materials and Methods

2.1. Material

[5] The material comes from five sites where cores were recovered by drilling offshore mid- and north Norway, between 63° and 74.5°N (Tables 1 and 2). The cores were taken in the course of the Foundation for Scientific and Industrial Research at the Norwegian Institute of Technology (SINTEF) Petroleum Research (formerly the Continental Shelf Institute (IKU)) "Shallow Drilling Project" between 1985 and 1991 [*Fjerdingstad et al.*, 1985; *Århus et al.*, 1987; *Skarbø et al.*, 1988; *Bugge et al.*, 1989; *Hansen et al.*, 1991]. The stratigraphic sections encompass the Oxfordian-Barremian interval.

[6] Figure 1 shows the location of the sites in their paleogeographic context. The sites are identified by a number-letter code. The first six digits are the lease block number, the letter refers to the type of hole, and the last two digits are the site number within the block. Of the first four digits of the site names, the first two are the latitude and the last two the longitude in degrees N and E. Figure 2 shows the lithology and stratigraphy of the sections. We examined a total of 491 samples to determine sediment petrography, inorganic and organic geochemistry, calcareous nannofossil, and foraminiferal content. Sample numbers indicate depth below seafloor.

2.1.1. 6307/07-U-02

[7] This site is located at 63°27′54.35″ N, 07°14′44.26″ E, offshore mid-Norway (off Smøla Island) in the southern part of the Hitra Basin. *Skarbø et al.* [1988] described the 190.1 m thick sequence as Quaternary sediments (0–13.6 mbsf) and an Early Cretaceous-Late Jurassic section of claystones and marls (13.6–190.1 mbsf) ranging in age from early Hauterivian/late Valanginian to early Volgian/late Kimmeridgian. The Mesozoic section can be subdivided into three lithologic units: (1) red and grey carbonate-cemented shale/claystones at the top (Lange Formation, early Hauterivian-late Berriasian, 13.6–36.4 mbsf) are underlain by (2) dark

Table 2. Lithology, CaCO3%, Stratigraphic Units, Age, and Type and Number of Samples Taken at Sites off Norway[a]

Depth in Hole, m	Lithology	$CaCO_3$, %	Stratigraphic Unit	Age	ISO	IGC	OGC	CN	F
				Site 6307/07-U-02					
0–13.6				Quaternary					
13.6–36.4	red and grey marls	0.5–31.7	Lange Fm.						
13.6–24.6		0.6–31.7		Early Valanginian	15	12	12	16	11
24.6–36.4		0.5–22.5		Earliest Valanginian-Latest Berriasian	6	13	13	18	22
36.4–104.8	dark claystones	0.2–17.2	Spekk Fm.	Late Berriasian-Early Volgian	2	46	46	33	47
104.8–183.5	fine-grained sandstones	2–8.5	Rogn Fm.	Early Volgian-Late Kimmeridgian		2			
183.5–190.1	dark clays		Spekk Fm.	Kimmeridgian					
				Site 7430/10-U-01					
0–10.5				Quaternary					
10.5–33.7	dark grey claystones	1.1	Kolje Fm.	Barremian		1	1	111	2
33.7–42.9	marly limestones	13.2–76.8	Klippfisk. Fm.	Early Barremian, Mid. Hauterivian-Early Valanginian-Late Berriasian	12	8	8	14	7
42.9–67.6	black shales	0.3–21.3	Hekkingen Fm.	Late Berriasian-Kimmeridgian	8	139	139	18	17
				Site 6814/04-U-02					
0–7.0				Quaternary					
7.0–39.83	dark grey mudstone	0.6–8.8	Kolje Fm.	Early Barremian		21	21		22
39.83–67.50	calcareous siltstone w. limestone nodules	1.1–47.8	Klippfis k Fm.	Hauterivian-Valanginian	19	18	18		27
67.50–191.25	dark claystones	0.7–13	Hekking en Fm.	Late Berriasian-	73	48	48		66
				Site 7425/09-U-01					
0–49.9				Quaternary					
49.9–53.5	grey claystones	0–4.0	Kolje Fm.	Early Barremian					
53.5–58.8	marly limestones	9.4–61.0	Klippfisk Fm.	Early Barremian-Early Valanginian				9	
58.8–63.7	brown claystones	1.7–25.0	Hekkingen Fm.	Early Valanginian				9	
63.7–64.4	green limestones			Earliest Valanginian-				6	
				Site 7231/01-U-01					
0–36.5				Quaternary					
36.5–59.8	dark grey claystones		Kolje Fm.	Barremian				29	
59.8–64.5	marly limestones	9.1–39.1	Klippfisk Fm.	Mid. Hauterivian-Early Valanginian				3	
65.5–93.0	dark grey clays		Hekkingen Fm.	Late Volgian-Late Oxfordian				23	

[a]where ISO = isotopic analyses, IGC = inorganic geochemistry; OGC = organic geochemistry, CN = calcareous nannoplankton, and F = foraminifera.

silt/claystones (Spekk Formation, late Berriasian-early Volgian, 36.4–104.8 mbsf), which in turn are underlain by (3) fine-grained sandstones (Rogn Formation, early Volgian-late Kimmeridgian, 104.8–183.5 mbsf). Dark clays at the base are again assigned to the Spekk Formation (Kimmeridgian, 183.5–190.1 mbsf). The age assignments of *Skarbø et al.* [1988], based on palynomorphs and foraminifera, have not been subsequently revised. Table 2 shows the lithologies, stratigraphic units, ages, and numbers of samples taken at this and the other sites.

2.1.2. 6814/04-U-02

[8] This site is located at 68°9′45.8″ N, 14°09′47.1″ E, offshore mid-Norway (off the Lofoten Islands) in the northern part of the Ribban Basin. *Hansen et al.* [1991], and *Smelror et al.* [2001a] have described the 191.25 m thick sequence, which consists of Quaternary sediments (0–7 mbsf) and an Early Cretaceous-Late Jurassic (7–191.25 mbsf) section consisting of claystones, limestones, siltstones, and mudstones. These sediments range in age from early Barremian to early Volgian. The Mesozoic section is comprised of three lithological units: (1) dark grey mudstones at the top (Kolje Formation, early Barremian, 7.0–39.8 mbsf) overlie a sequence of (2) alternating calcareous siltstone and limestone nodule-bearing beds (Klippfisk Formation, Hauterivian-Valanginia, 39.8–67.5 mbsf), underlain by (3) dark claystones at the base (Krill Member of the Hekkingen Formation, late Berriasian-early Volgian, 67.5–191.2 mbsf). The age assignments, based on palynomorphs, foraminifera, and macrofossils [*Hansen et al.*, 1991; *Smelror et al.*, 2001a] have not been subsequently revised.

2.1.3. 7430/10-U-01

[9] This site is located at 74°12′47.79″ N, 30°14′44.22″ E on the central part of the Barents Sea Shelf, Bjarmeland Platform. *Bugge et al.* [1989], *Århus* [1991], and *Smelror et al.* [1998] have described the 67.6 m of sediment cored, which consists of Quaternary sediments (0–10.5 mbsf) and an Early Cretaceous-Late Jurassic section of upper Barremian to Kimmeridgian claystones and marls (10.5–67.6 mbsf). The Mesozoic section can be subdivided into three units: (1) dark grey claystones at the top (Kolje Formation, Barremian, 10.5–33.7 mbsf) are underlain by (2) marly limestones (Klippfisk Formation, early Barremian to late Berriasian, 33.7–42.9 mbsf, with hiatuses between the early Valanginian and middle Hauterivian and the latter and early Barremian parts of the section. The basal part of the section is characterized by (3) laminated black shales of the Hekkingen Formation (late Berriasian-Kimmeridgian, 42.9–67.6 mbsf).

[10] Using palynomorphs and calcareous nannofossils, *Smelror et al.* [1998] modified the earlier age assignments of *Bugge et al.* [1989]. Their modified zonation is followed here. This site is only 46 km from the center of the Mjølnir

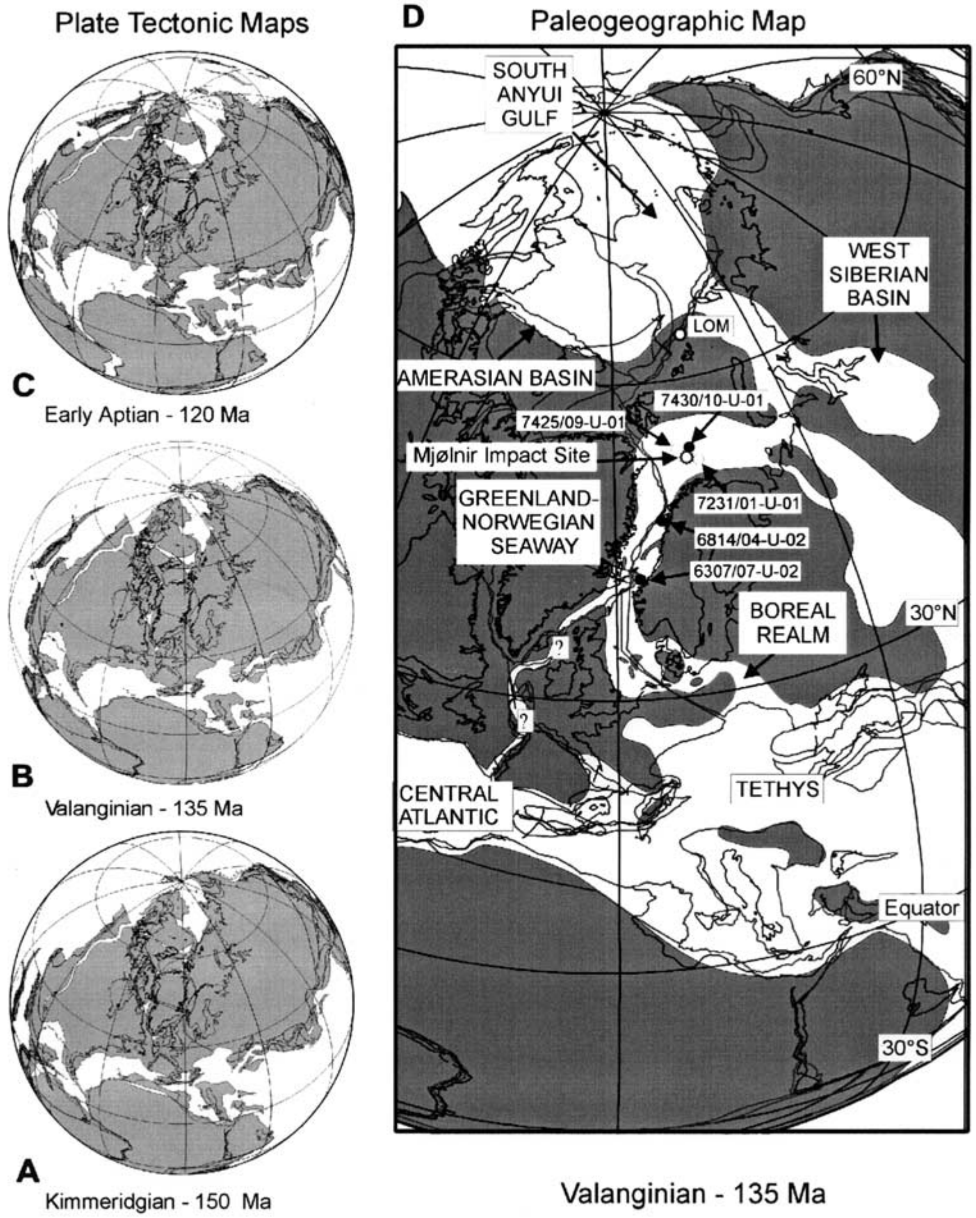

Figure 1. Globes showing plate tectonic configurations for (a) 150 Ma (early Tithonian), (b) 135 Ma (Valanginian), and (c) 120 Ma (early Aptian). Continental bocks and terranes in grey; ocean crust in white; only present shorelines are indicated. (d) Paleogeographic map for the Valanginian from Africa to the Arctic, showing transcontinental seaways, major marine embayments and basins, and the sites on the Norwegian shelves.

Meteorite impact site (73°50′ N, 29°40′ E), which has a diameter of 40 km [*Gudlaugsson*, 1993; *Dypvik et al.*, 1996]. Cores from two additional sites were sampled only for calcareous nannofossils.

2.1.4. 7231/01-U-01

[11] This site is located at 72°45′12.45″ N, 31°07′30.21″ E in the central part of the Barents Sea Shelf, the Nordkapp Basin. *Århus et al.* [1987], *Århus* [1991], and *Smelror et al.* [1998] have described the 93 m of sediments, with Quaternary (0–36.5 mbsf) cover on lower Barremian to Kimmeridgian/Oxfordian claystones and marls (36.5–93 mbsf). The age assignments followed here are based on palynomorphs [*Århus*, 1991].

2.1.5. 7425/09-U-01

[12] This site is located at 74°29′25.30″ N, 25°46′19.30″ E on the northwestern part of the Barents Sea Shelf, on the western Bjarmeland Platform. *Fjerdingstad et al.* [1985], *Århus et al.* [1990], *Århus* [1991], and *Smelror et al.* [1998] have described the 64.4 m section, which consists of Quaternary sediments (0–49.9 mbsf) and early Barremian to late Berriasian claystones and marls (49.9–64.4 mbsf). The original age assignments of *Fjerdingstad et al.* [1985]

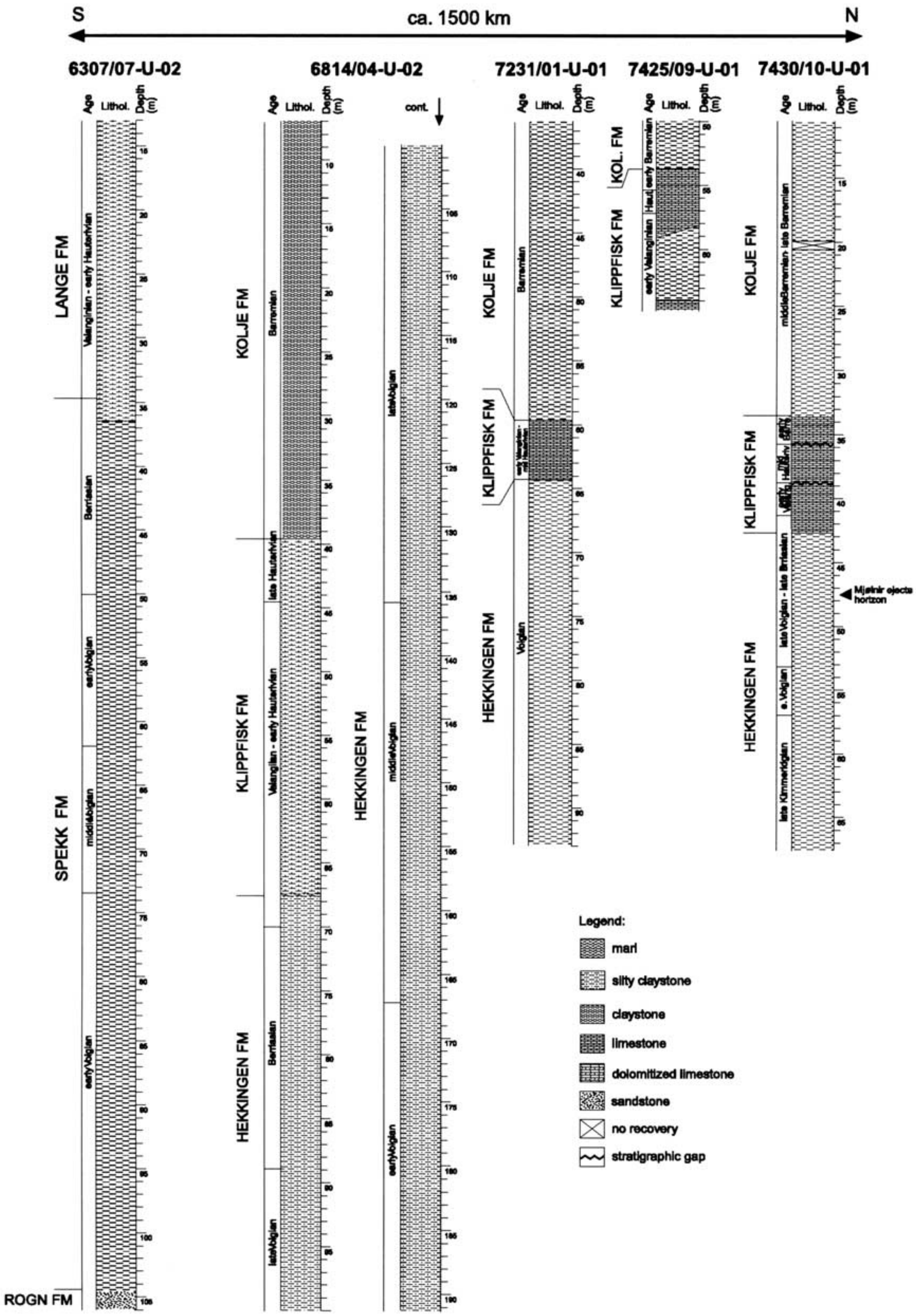

Figure 2. Lithology and stratigraphy of the sections on the Norwegian shelves.

were revised by *Smelror et al.* [1998] using palynomorphs and calcareous nannofossils. Their age determinations are followed here.

2.2. Methods

2.2.1. Sedimentology

[13] The cyclic bedding patterns in cores from Sites 6307/07-U-02, 6814/04-U-02 and 7430/10-U-01 were investigated with a spectrophotometer (Minolta, CM 2002). Sampling at 1 cm resolution was possible on all cores except those affected by disintegration (e.g., Site 6307/07-U-02, 13–65 m). The measured L* value is based on a relative scale from 0 to 100% and is a function of the lightness of the lithology. It is expressed as a grey value between the end-members, black and white. Correlations of L* to the amount of carbonate/dolomite and L*/TOC show that in calcareous sections the L* value is a good estimate for the amount of carbonate. However, in shaly units, L* is inversely correlated with the total organic carbon (TOC) content [see *Nebe*, 1999].

[14] The lightness data set, consisting of more than 22,000 measurements made at 1 cm intervals, was analyzed using ‘‘speclab’’ [*Port*, 2001], a spectral analysis program based on the Lomb-Scargle algorithm [*Lomb*, 1976; *Scargle*, 1982]. The size of the sampling interval is well below the Nyquist frequency of the basic cycles, which typically have a thickness of 20–30 cm. There was no filtering or other modification of the data set prior to the spectral analysis.

2.2.2. Inorganic Geochemistry

[15] A total of 308 samples from Sites 6307/07-U-02, 6814/04-U-02, and 7430/10-U-01 were homogenized in an agate mortar. The ground material was used for all geochemical analyses. All samples were analyzed for major elements (Ti and Al) and trace metals (As, Cr, Cu, Mo, Ni, V, Zn, and Zr) by X-ray fluorescence (XRF) (Philips PW 2400, equipped with a Rh tube) using fused borate glass beads. Total sulfur (TS) and total carbon (TC) for all samples were determined after combustion using an IR-analyzer LECO SC-444. Total inorganic carbon (TIC) was determined in 184 samples by a Coulometrics Inc. CM 5012 CO_2 coulometer coupled to a CM 5130 acidification module [*Huffmann*, 1977; *Engleman et al.*, 1985]. The content of TOC was calculated as the difference of TC and TIC. Selected trace metals (Cr, Cu, Mo, Ni, and U) were analyzed in 94 samples by inductively coupled plasma mass spectrometry (ICP-MS) (Finigan MAT Element) after acid digestion [*Heinrichs and Herrmann*, 1990; *Heinrichs et al.*, 1986]. Precision and accuracy of XRF and ICP-MS measurements were tested by replicate analysis of international geological reference materials (e.g., GSD-4, -9, and -10) and several ‘‘in-house’’ standards. The precision of bulk parameter measurements [*Prakash Babu et al.*, 1999] was checked in series of double runs. Accuracy was determined by using in-house standards.

2.2.3. Organic Geochemistry

[16] A total of 306 samples from Sites 6307/07-U-02, 6814/04-U-02, 7430/10-U-01 were analyzed using geochemical and petrographical methods to quantify the amount and determine the genetic type of the organic matter in order to characterize the depositional setting. This includes 122 samples from a high-resolution analysis of cores from Site 7430/10-U-01. Geochemical methods include the determination of TC, total nitrogen (TN), total sulphur (TS), and TOC using LECO CNS-2000, CS-400 and CS-125 instruments, respectively. Rock-Eval pyrolysis was applied to all samples to estimate the quantity, quality, and thermal maturity of the organic matter indicated by the hydrogen index (HI), oxygen index (OI), and T_{max} (temperature of maximum hydrocarbon liberation during pyrolysis). We used a Rock-Eval II device and IFP 55000 standards. Two standards were measured every 10 samples, yielding an analytical precision of ″10% for S2 (HI), ″15–20% for S3 (OI), and ″2°C for T_{max} values. Results were plotted in a van-Krevelen diagram to determine the different kerogen types (I = highly oil prone to IV = inert) and classify the genetic sources of the organic matter, e.g., terrigenous versus marine [*Espitalié et al.*, 1977; *Tissot and Welte*, 1984; *Peters*, 1986], and were subsequently confirmed by microscopic examination. For a detailed study of the composition of the organic matter, we conducted microscopic determinations of the macerals (individual constituents of solid organic matter) using polished blocks from whole rock samples examined under reflected white and UV light [following *Taylor et al.*, 1998]. The quantitative optical analysis was performed on a Zeiss microscope by point counting using an ocular with a 20 point cross hair grid. Photographs were taken with a Zeiss Axiocam digital camera. With information about the type, composition, and degree of preservation of the organic matter (OM) it is possible to describe the depositional conditions in terms of transport path (long/short), environment of accumulation (energetic/stagnant), degree of bottom water oxygenation, sources (marine, brackish, terrestrial), and climate (e.g., fusinites = arid; gelovitrinite = humid).

2.2.4. Calcareous Nannofossils

[17] A total of 290 smear-slide preparations of material from Sites 6307/07-U-02, 7425/09-U-01, 7430/10-U-01 and 7231/01-U-01 were examined under a light microscope using a magnification of 1500 times. Calcareous nannofossils constitute 0–20% of the whole rock. The species abundance for each sample was determined by counting at least 300 specimens or all specimens in at least 200 fields of view. Preservation is indicated as follows: E1 (slightly etched), E2 (moderately etched), and E3 (heavily etched). Although it occurs, overgrowth was not reported. Bibliographic references for the taxa are given by *Perch-Nielsen* [1985] and *Bown* [1998].

2.2.5. Foraminifera

[18] A total of 222 washed samples from cores taken at Sites 6307/07-U-02, 6814/04-U-02, and 7430/10-U-01 were analyzed with a binocular using a magnification of 185 times. Dried sediment samples were processed with tenside (REWOQUAT ® W 3690 PG) since the standard hydrogen peroxide method was not efficient. After crushing, the sample was covered with a tenside/ethanol mixture. Several times a week the sample was stirred up. After one to two weeks the sample was washed through a 200 μm and a 63 μm sieve. The insoluble material was weighted and sub-

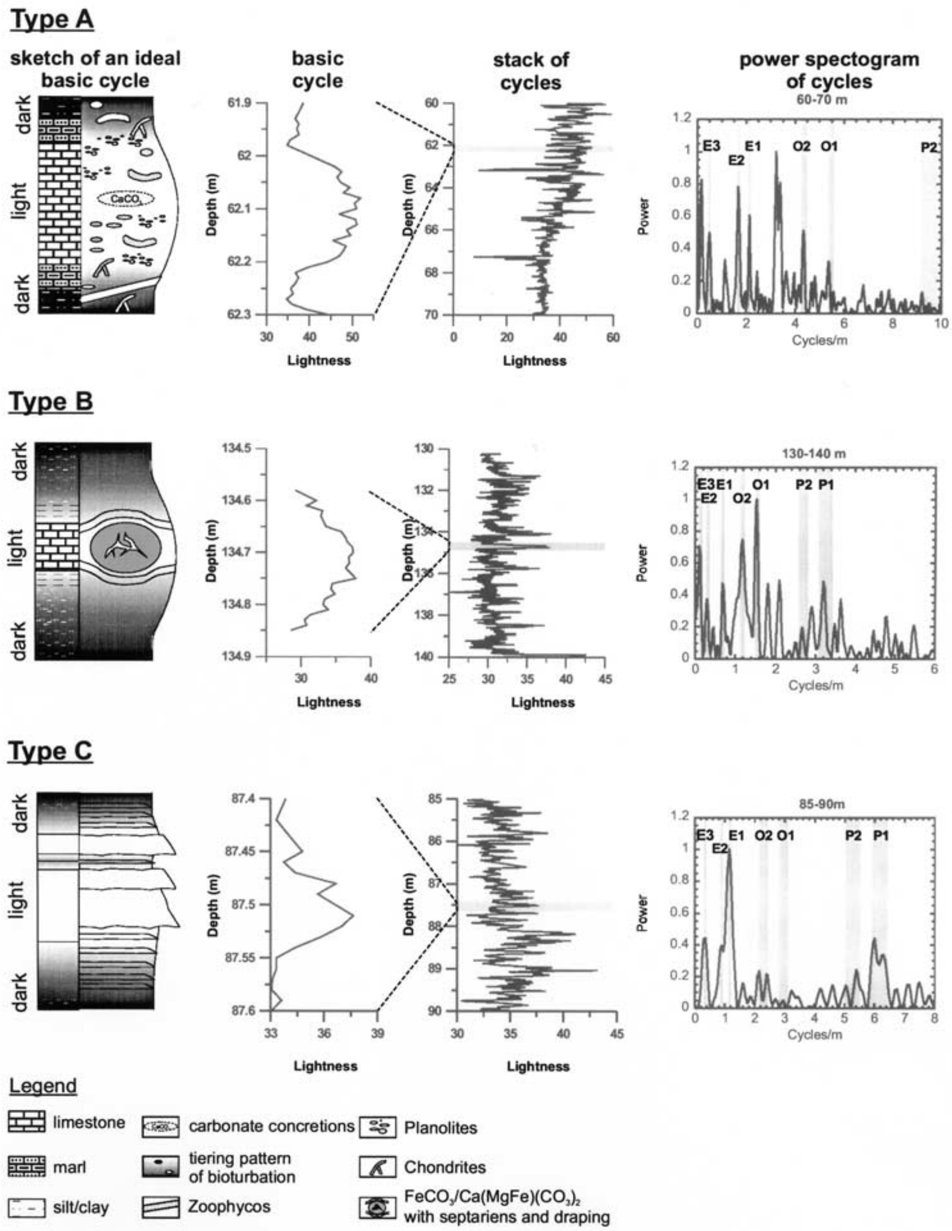

Figure 3. Schematic diagram of three characteristic types of bedding cycles, high-resolution lightness logs with equivalent power spectra and idealized lithologies. Type A cycles are expressed by variation in the carbonate content and the bioturbation pattern, and Type B cycles indicate alternations between black shales and siderite/dolomite concretions. Type C cycles are alternations between black shales and pulses of silt dilution. Type A and B cycles are from Site 6814/04-U-02, and Type C cycle is from Site 6307/07-U-02.

tracted from the original weight of the sample. After drying and weighing, the sample was sieved in three fractions (>315, 200–315, 100–200, and <100 μm). The fractions were picked qualitatively and quantitatively, if necessary splits were made. At least 300 individuals were picked in each sample. The generic classification we follow is based primarily on *Loeblich and Tappan* [1987]. Classification at species level is based on a wide range of literature [e.g., *Bartenstein and Brand*, 1951; *Holbourn and Kaminski*, 1997; *Nagy and Basov*, 1998].

3. Results

3.1. Sedimentology

[19] Three major kinds of sedimentary cycles, termed Types A, B, and C, can be differentiated (Figure 3). Each

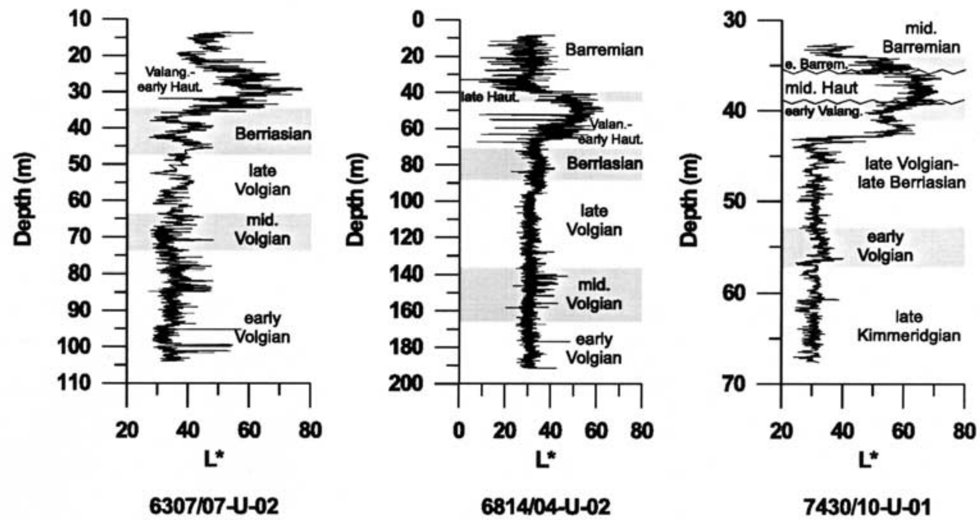

Figure 4. Lightness logs (L*) of cores from sites 7430/10-U01, 6814/04-U-02, and 6307/07-U-02. The resolution of lightness measurements was 1 cm unless cores were affected by a high degree of disintegration. Frequency analysis, applying the Lomb-Scargle algorithm to the non filtered lightness data, suggests that sedimentation was influenced by orbital parameters.

is characteristic of successive stratigraphic levels, from the early Volgian to the early Hauterivian (Figure 4). The differentiation of these cycle types is based on differences in lithology, degree of bioturbation, and related color changes.

[20] Type A cycles are characterized by bed-scale changes in carbonate content from 5 to 45%. Strongly bioturbated carbonate-rich intervals alternate with fewer bioturbated shaly intervals. The carbonate-rich intervals commonly display *Planolites*-like structures. The carbonate-poor intervals, which are slightly richer in organic carbon, contain *Zoophycos* and *Chondrites* ichnofossils, suggesting oxygen-deficient conditions [*Savrda and Bottjer*, 1989]. The white and dark infill structures at the base and the top of these cycles suggest that sedimentation was continuous. The carbonate-rich intervals may contain $CaCO_3$ nodules or concretions (i.e., 6814/04-U-02, 41–64 m). Type A cycles are observed in the Valanginian-Hauterivian section at Sites 6307/07-U-02 (20–36 m), 7430/10-U-01 (34–44 m), and 6814/04-U-02 (40–67 m).

[21] Type B cycles are dominated by laminated TOC-rich black shale layers. Intercalated layers may contain siderite and ankerite concretions or concretionary layers. There are some large concretions (up to ~15 cm in diameter) that show draping, indicating that they formed prior to compaction. Some siderite and ankerite concretions are characterized by late diagenetic blocky calcite fills, representing shrinking veins. Bundling is expressed by stacking of layers with smaller concretions. The distribution of concretions seems to follow primary depositional layers. Type B cycles containing concretions occur at Site 6814/04-U-02 from 9 to 40 m, from 122 to 152 m, and at Site 7430/10-U-01 from 43 to 56 m. Cycles of Type B lacking concretions are observed at Site 6307/07-U-02 from 37 to 84 m, at Site 6814/04-U-02 from 98 to 122 m and from 160 to 192 m, and at Site 7430/10-U-01 from 48 to 56 m. The cyclicity in the laminated black shale sections is characterized by a faint color variation. Site 6814/04-U-02 contains a transition from Type B to Type A cycles between 68 and 98 m.

[22] Type C cycles occur in the siliciclastic-dominated sequences at the base of the sections at Sites 6307/07-U-02 and 7430/10-U-01. They are characterized by a succession of small-scale graded event beds consisting of silt/mud couplets. The silty layers dilute the TOC-rich background. Individual event beds range from 2 to 10 cm in thickness. Each event bed is composed of faint lamination and occasionally shows scouring at the base. The event beds are grouped into bundles of 4 to 8. Thicker siliciclastic events are associated with lighter colors and lower TOC content. These cycles may reflect facies-related autocyclic processes [*Einsele*, 2000]. They are easily recognized by color changes by the spectrophotometer and well expressed in spectral analysis. At Site 7430/10-U-01, from 56 to 68 m, Type C cycles are fine-grained whereas at Site 6307/07-U-02, from 85 to 104 m, they are coarser-grained. The former are interpreted as being more distal from, and the latter more proximal to, the source.

[23] Each cycle type is characterized by a distinctive color variation. Type A and Type B cycles have L* values from 30 to 60 and from 25 to 37, respectively. Type C cycles show L* values from 30 to 40. Although the various cycle types have a different origin, all of them show bundling with 3 to 6 cyclic beds per bundle (see Figure 3), suggesting a hierarchical pattern in cyclicity. The bundles reflect variations in the carbonate content (Type A), stacked concretion beds (Type B), or siliciclastic events (Type C).

3.2. Inorganic Geochemistry

[24] Samples from the southern site (6307/07-U-02) differ from the more northerly sites (6814/04-U-02 and 7430/10-U-01) in their major element ratios. Ti/Al ratios at the individual sites are significantly different (Figure 5a). Sam-

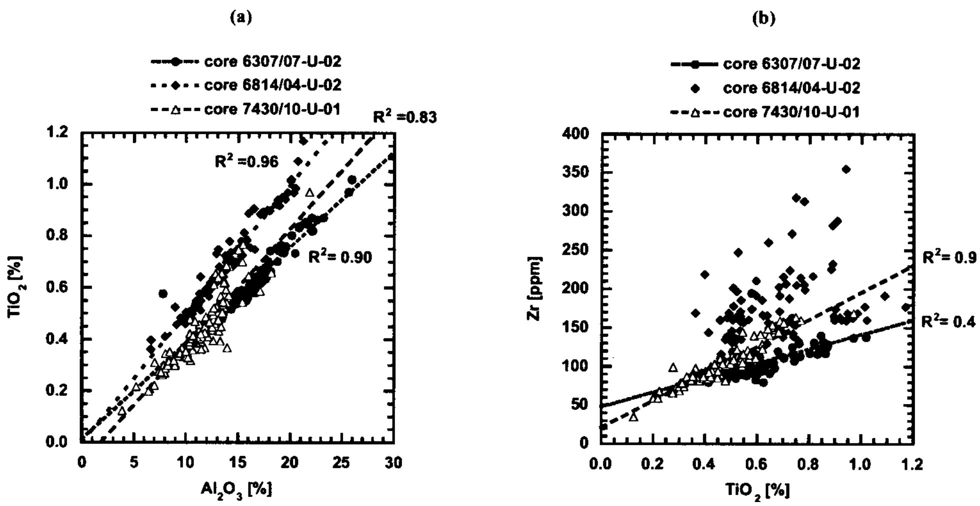

Figure 5. (a and b) Ti/Al and Zr/Ti ratios of samples from 6307/07-U-02, 6814/04-U-02, and 7430/10-U01.

ples from Sites 6307/07-U-02 and 7430/10-U-01 exhibit Ti/Al ratios lower than those at Site 6814/04-U-02. Regarding Zr as a proxy for heavy minerals such as zircon, the higher Zr/Ti ratios in samples from Sites 6307/07-U-02 and 7430/10-U-01 compared to samples from Site 6814/04-U-02 (Figure 5b) suggests that the sediments at the latter must have been transported from shallower and/or more energetic depositional environments.

[25] Redox-sensitive and stable sulfide-forming trace metals (e.g., As, Cr, Cu, Mo, Ni, U, V, and Zn) are significantly enriched in layers with TOC contents exceeding 5% (Figure 6). The high Zn values at Site 7430/10-U-01 can only be explained by assuming an additional metal source, most likely hydrothermal activity. Except for As and Cr, trace metal enrichments are much lower at Site 6814/04-U-02 than at Sites 6307/07-U-02 and 7430/10-U-01.

[26] Paleoceanographic changes may be understood by comparing the variation in Mo/Al ratio in each section (Figures 7a–7d). At Site 6307/07-U-02 the Mo/Al ratios vary from <0.2 to 25 $\times 10^{-4}$, with maximum values between 77 and 92 mbsf. At Site 6814/04-U-02, Mo/Al ratios are significantly lower (<0.2–9.7 $\times 10^{-4}$). Most values in the

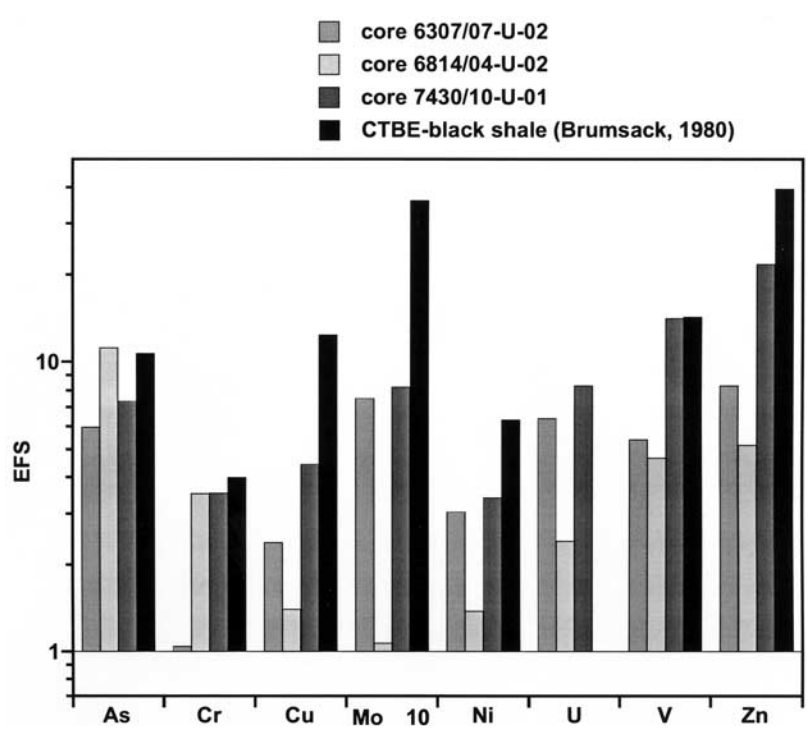

Figure 6. Enrichment factors, relative to average shale (($element_{sample}/Al_{sample}$)/($element_{av.shale}/Al_{av.shale}$)), for redox-sensitive elements in samples from 6307/07-U-02, 6814/04-U-02, and 7430/10-U01.

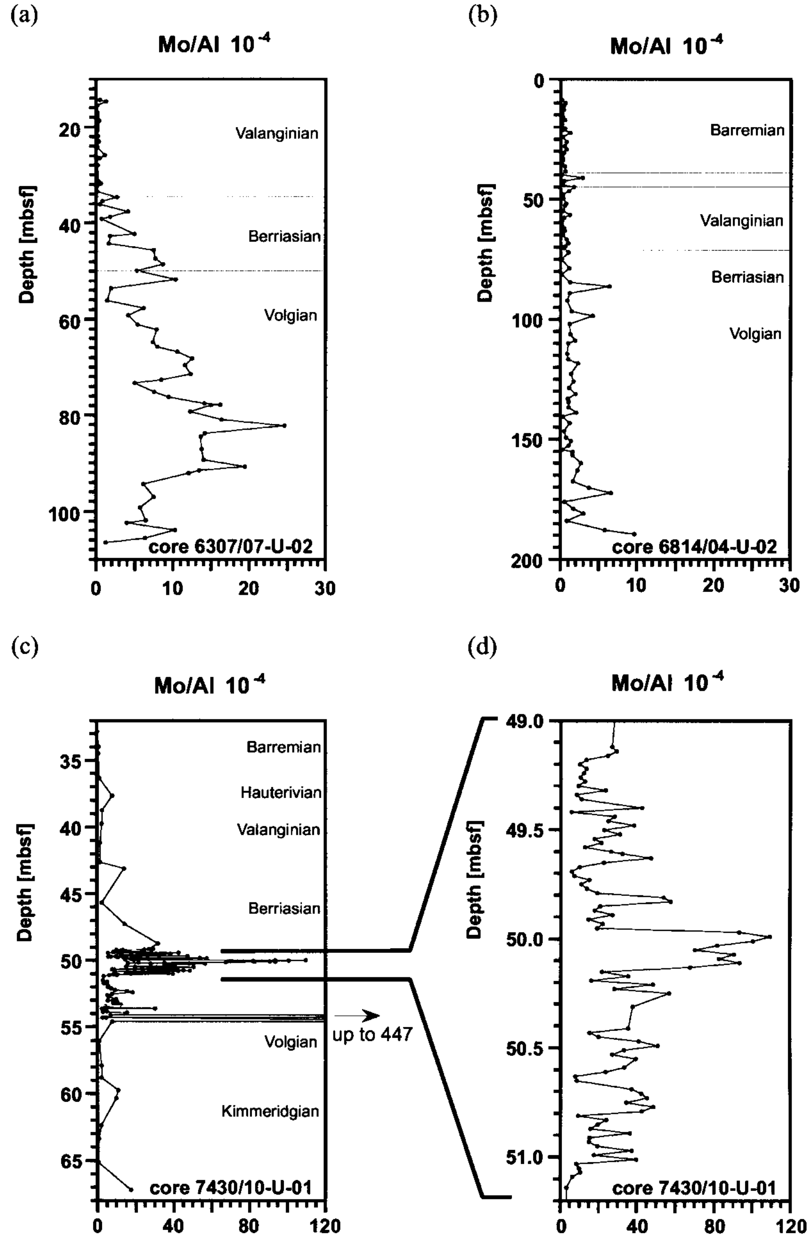

Figure 7. (a–d) Mo/Al ratios of samples from 6307/07-U-02, 6814/04-U-02 and 7430/10-U-01.

upper part of the section do not differ significantly from average shale. The highest Mo enrichments occur in samples from Site 7430/10-U-01, where Mo/Al ratios range from 0.1 to 447 $\times$ 10^{-4}.

3.3. Organic Geochemistry

[27] The TOC values in samples from offshore mid-Norway and the Barents Sea are comparable to many other Cretaceous black shales reported from lower palaeolatitudes [e.g., *Arthur et al.*, 1987; *de Graciansky et al.*, 1987], except for core 7430/10-U-01, which has extraordinarily high values (Figure 8).

[28] Values for TOC in the Spekk Formation at Site 6307/07-U-02 average 4.5″ 2.5 wt % and decrease toward the top of the unit. Similar values continue into the base of the overlying Lange Formation but then abruptly drop below 1.0 wt % and approach 0% above 26 mbsf. Hydrogen index (HI) values vary widely, from 200 to 600 mg HC/g TOC, but indicate a significant contribution of marine- and/or lipid-rich terrigenous organic matter. The mean HI values decrease slightly from 450 to 350 mg HC/gTOC from bottom to top. Both TOC and HI correlate well (0.77), suggesting that preservation was the major factor controlling black shale formation. T_{max} values range from 400°C to 425°C within the Volgian sequences, indicating thermally immature organic matter with an excellent oil-prone petroleum source rock potential with predominantly type II and II/III kerogens.

[29] Highly variable TOC values of 3.0″ 2.0 wt % characterize the Hekkingen Formation at 6814/04-U02. The

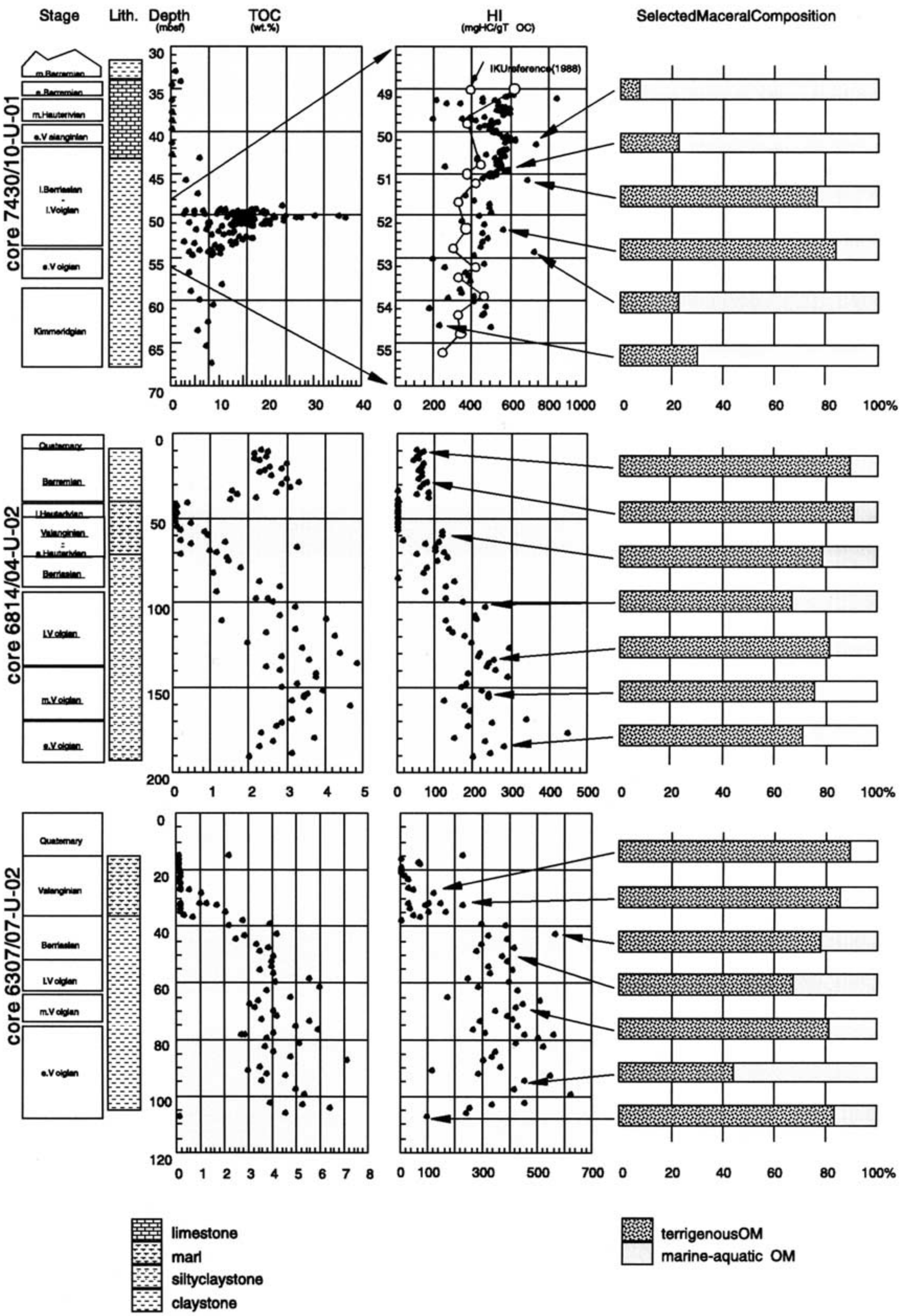

Figure 8. TOC, hydrogen index, and organic matter composition in samples from 6307/07-U-02, 6814/04-U-02, and 7430/10-U-01.

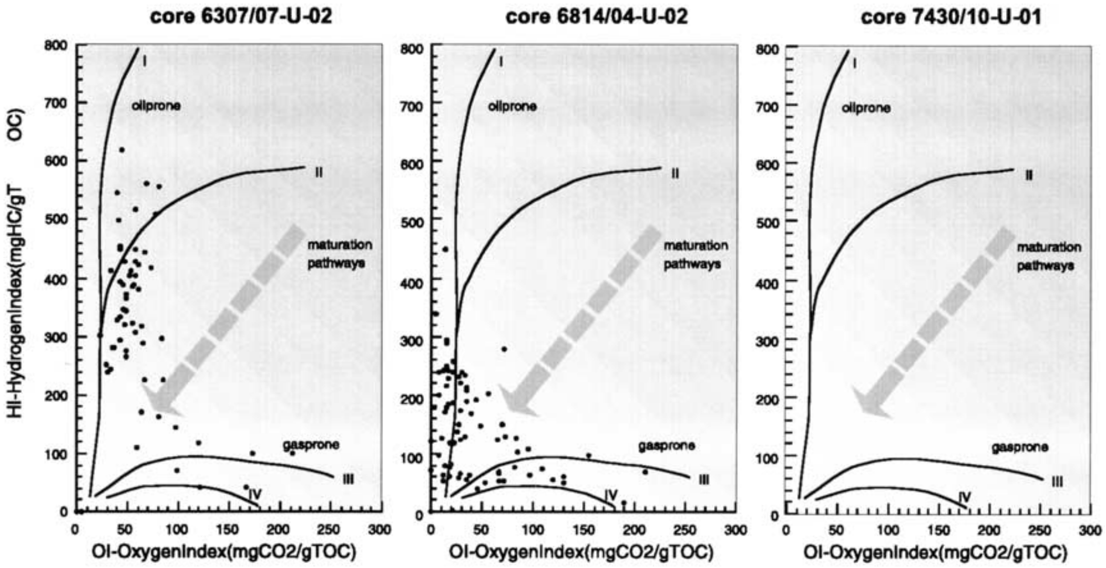

Figure 9. Van Krevelen diagrams for hydrogen and oxygen indices for samples from 6307/07-U-02, 6814/04-U-02, and 7430/10-U-01.

coarser-grained calcareous Klippfisk Formation is almost barren of organic carbon, but the overlying Kolje Formation has TOC values of 2.5″ 1.0 wt %. As shown in Figure 9, samples from the Hekkingen Formation have HI values ranging from 50 to 450 mg HC/gTOC. HI values decrease substantially to <100 mg HC/gTOC toward the top of the unit. The organic matter is type II/III to III kerogen with a good oil/gas-prone petroleum source rock potential. Most of the Klippfisk Formation is barren. The Kolje Formation shows HI values of 40–70 mg HC/gTOC with a mean of 55 mg HC/gTOC and low variability. HI/OI ratios indicate slightly mature organic matter of type III and IV kerogen.

[30] The highest TOC values occur at the northernmost Site 7430/10-U01 (Figure 8), ranging from 3.6 to 36 wt % within the Hekkingen Formation, and with a marked increase from 49 to 52 mbsf. The sequence is characterized by thermally immature organic matter with hydrogen indices ranging between 200 and 600 mg HC/gTOC, delivering type I and II kerogen with an excellent oil-prone hydrocarbon generative potential (Figure 9). Earlier analyses by IKU laboratories at a lower stratigraphic resolution produced less variable but similar values. We found some intervals of significantly elevated HI values which coincide with element enrichments, e.g., molybdenum. The overlying Klippfisk Formation is extremely poor in TOC, similar to the Lange Formation at Site 6307/07-U02 and the Klippfisk Formation at Site 6814/04-U02. In the uppermost Kolje Formation, TOC values are 0.9–1.9 wt %, and HI values range from 27 to 47 mg HC/gTOC. The organic matter appears to be primarily of terrigenous origin.

3.4. Micropaleontology

[31] The nannofossil assemblages generally have a low diversity. Of the 40 species encountered, the most common include *Watznaueria barnesae*, *Crucibiscutum salebrosum*, *Biscutum constans*, and *Rhagodiscus asper*. Together, they make up ~80–90% of the assemblages (Figure 10). *C. salebrosum*, which is rare or absent at low latitudes, is extremely common in the Norwegian samples. Other common taxa include *Cyclagelosphaera margerelii*, *Diazomatolithus lehmanii*, *Microstaurus chiastius*, *Rotelapillus laffittei*, *Sollasites horticus*, *Vekshinella stradneri*, and *Zygodiscus spp*. Diversity (equal to number of species) varies from 7 to 25 species/sample; 10–20 species/sample are more often encountered. The marly, carbonate-rich sediments of the earliest Cretaceous (early Valanginian and mid Hauterivian) have higher diversities than those of the Barremian. A comparison of the four nannofossil-bearing cores shows a distinctive decrease of diversity from south to north: 15–25 species were observed in the southernmost core 6307/07, 7–13 species in core 7425/09, and 11–15 species in the northernmost core 7430/10. A comparison of abundance in individual time slices also indicates that diversity is controlled by palaeogeography. Early Valanginian assemblages, which were encountered in three cores, show a decrease of diversity from south to north.

[32] The foraminiferal assemblages are similar at all of the sites. Figure 11 shows the species abundances at 6307/07-U-02. Foraminiferal diversities and abundances are moderate in samples with high TOC values, and samples with more than 6% TOC contain no foraminifera at all (Site 6307/07-U-02 below 48.51 mbsf and Site 7430/10-U-01 below 42.62 mbsf). *Haplophragmoides*, *Recurvoides*, and *Evolutionella* occur in the C_{org}-rich muds at these sites, but no calcareous foraminifera occur in this interval. A distinctive flood of *Evolutionella* and *Recurvoides* occurs in earliest Cretaceous samples from Site 6307/07-U-02 (off mid-Norway). At Site 6814/04-U-02, low-C_{org} samples of Volgian age also contain agglutinated foraminifera. As the sedimentation from Volgian/Berriasian to Hauterivian changed from dark mudstones to grey carbonate-rich marls, the foraminiferal assemblages became more diverse. A number of calcareous foraminifera (mainly *Lenticulina*, *Globulina*, and *Laevidentalina*) occur in the Valanginian to Hauterivian strata. Radiolaria were

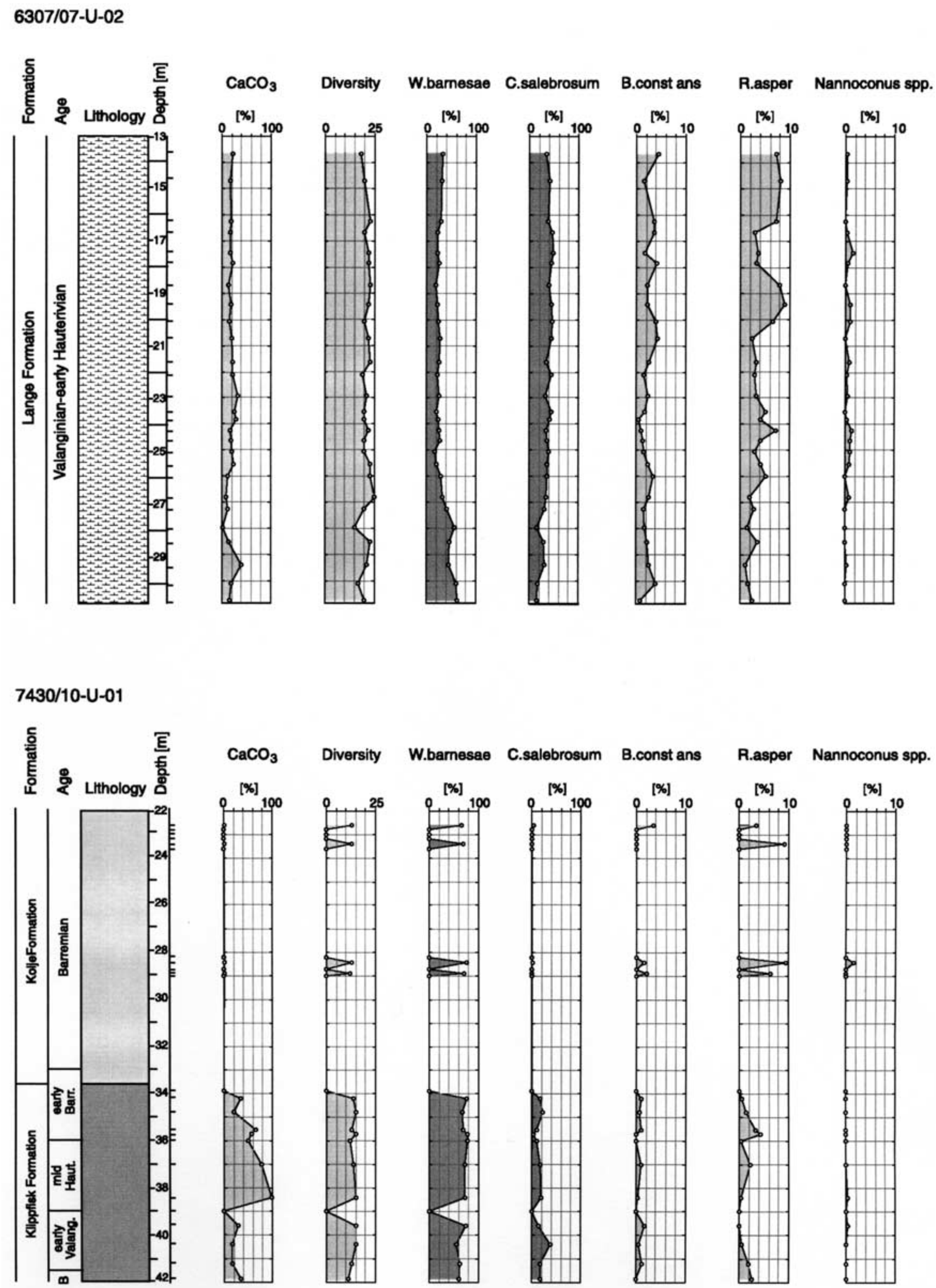

Figure 10. Abundances of calcareous nannoplankton species in the sections at 6307/07-U-02 and 7430/10-U-01 [from *Mutterlose and Kessels*, 2000].

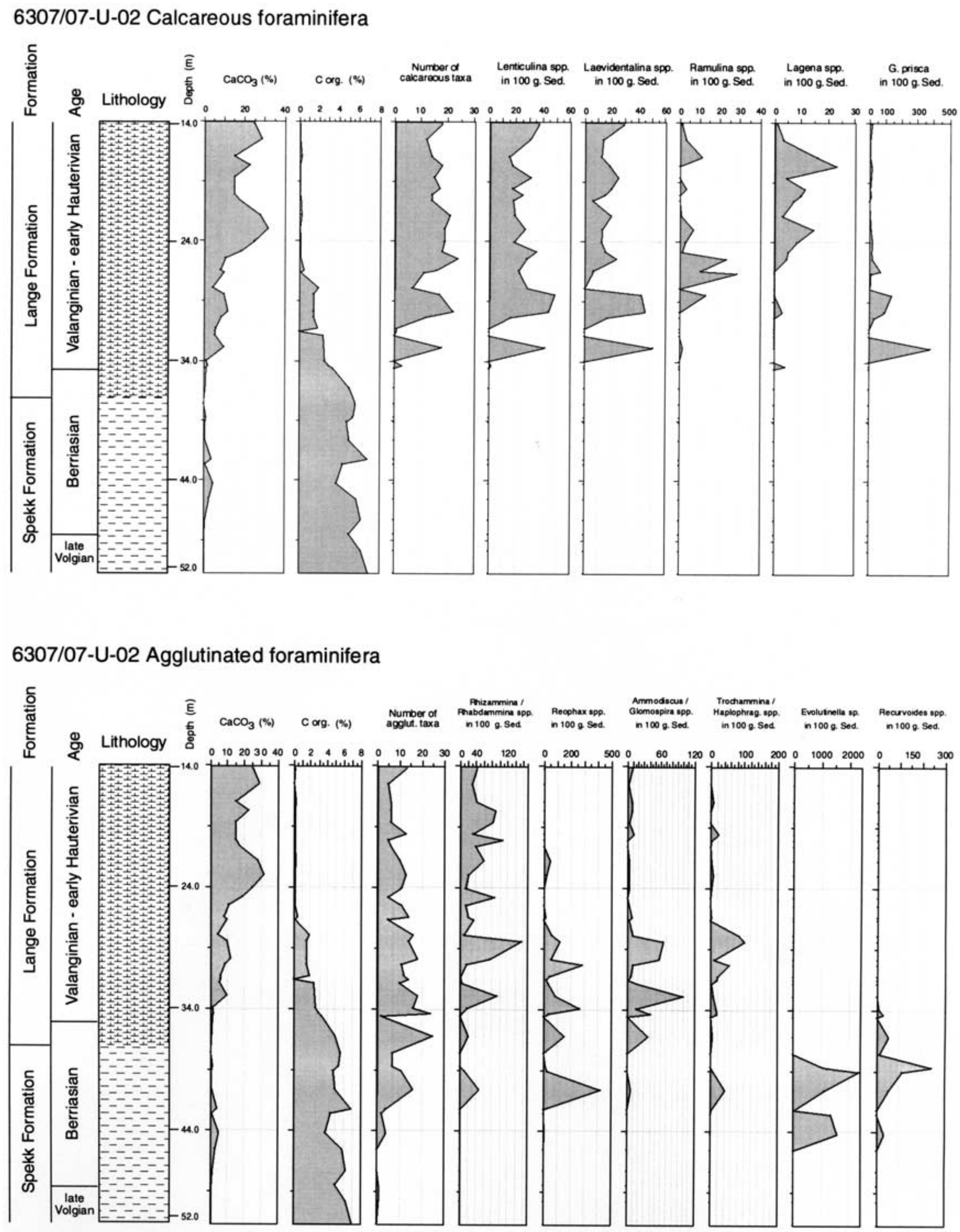

Figure 11. Abundances of calcareous and agglutinated foraminifera at 6307/07-U-02.

found at Sites 6307/07-U-02 and 7430/10-U-01 but have not been identified.

4. Discussion

[33] In order to evaluate the significance of the information from the sites in the Greenland-Norwegian Seaway, it is necessary to understand their location in a plate tectonic and paleogeographic context. Then the observations on the sediments and biota can be placed into a larger regional context. Finally, the new data can be interpreted in terms of the paleoclimate and paleoceanography of the Late Jurassic-Early Cretaceous.

4.1. Plate Tectonic and Paleogeographic Framework

[34] The plate tectonic framework locates the sites in terms of paleolatitude and nature of the surrounding crustal blocks. It forms the basis for reconstructing paleogeography.

Table 3. Present Locations, Paleolatitudes, and Distances Between Sites off Norway

Site	Present Latitude	Present Longitude	150 Ma Paleolatitude	135 Ma Paleolatitude	120 Ma Paleolatitude	Great Circle Distance From 6307/07-U-02, km
6307/07-U-02	63.28°N	7.25°E	42°N	43°N	45°N	0
6814/04-U-02	68.66°N	14.16°E	47°N	48°N	50°N	316
7430/10-U-01	74.21°N	30.24°E	54°N	55°N	56°N	1111
7425/09-U-01	74.49°N	25.77°E	54°N	53°N	56°N	1020
7231/01-U-01	72.75°N	31.12°E	53°N	52°N	54°N	1065
LOM-94-PC27	89°N (actual) 82.33°N (rotated)	149°E (actual) 80.41°E (rotated)	66°N	66°N	67°N	2392 (rotated)

[35] To determine the paleolatitude of a site, it is necessary to have a plate tectonic reconstruction and a reference frame for latitude and longitude. For our reconstructions (Figures 1a–1c) we have used the continental block outlines and plate rotations of *Hay et al.* [1999] (available at http://www.odsn.de), with modification of the Arctic as described below. We used the paleomagnetic reference frame of *Harrison and Lindh* [1982]; a hot spot reference frame would place sites 1–2° further north. Paleolatitudes of the sites are shown in Table 3.

[36] Reconstruction of the Tethys is complex and controversial. Currently, two different schemes are widely used, that of *Dercourt et al.* [1986, 1992], which was incorporated into the *Hay et al.* [1999] model used here, and an attractive new model by *Stampfli et al.* [2001]. Opening of the central Atlantic, between the U.S. margin of North America and northwest Africa started in the Jurassic, but opening between Iberia and the Grand Banks, first took place about 130 Ma, in Valanginian time (see plate tectonic maps in the work by *Hay et al.* [1999] or at http://www.odsn.de). The separation of Hatton and Rockall Banks from Greenland and from each other did not take place until the Late Cretaceous (80 Ma).

[37] Although the later plate tectonic history of the North Atlantic and Greenland-Iceland-Norwegian (GIN) Seas is relatively well known [*Wold*, 1995], the Late Jurassic-Early Cretaceous history of this region is uncertain. The northern North Atlantic (GIN) seas did not exist during the Mesozoic. Greenland formed a continuous unit with Scandinavia, sharing the Caledonian orogenic belt that had been formed in the Paleozoic. Although stretching along the boundary between Greenland and Norway began in the Late Cretaceous (about 80 Ma), the separation of the two did not occur until 58 Ma [*Hay et al.*, 1999].

[38] The Labrador Sea began to open during the Cretaceous Magnetic Quiet Interval, probably at 115 Ma, and ceased opening in the Oligocene, at about 33 Ma. It is unlikely that there was a North Atlantic-Arctic connection between North America and Greenland during the Early Cretaceous.

[39] Reconstruction of the Arctic is controversial, but its configuration is important for testing paleoclimatic and paleoceanographic hypotheses. The present Arctic Basin is bordered on the east by the Scandinavian Shield of Europe and Siberian Shield of Asia. On the west it is bordered by the Laurentian Shield of North America. Between these shields are smaller continental blocks of Greenland, the Canadian Arctic Islands, and the complex terrane regions of Alaska and eastern Siberia. Motions occurred between all of these units during the Mesozoic and Cenozoic. Those on the European-Greenland-North American side responded to the opening of the northern North Atlantic, and those on the Siberian side responded to the collisions of terranes arriving from the Pacific. Even taking into account crustal shortening associated with collisions, the blocks surrounding the present Arctic are not large enough to fill the space between North America, Greenland, and Eurasia during the Jurassic and Cretaceous. *Churkin* [1970] and *Churkin and Trexler* [1980] proposed that part of the Arctic Basin is an isolated piece of Pacific Ocean crust. Current speculation is that there was a polar ocean basin which has since been subducted. This ancient ocean basin is thought to be represented by the ophiolites of the South Anyui Terrane of northeastern Siberia. The hypothetical ocean is termed the "South Anyui Ocean," and the paleogeographical feature is the "South Anyui Ocean Gulf" [*Kazmin and Napatov*, 1998].

[40] The modern Arctic Ocean consists of two deep basins, separated by the long narrow Lomonosov Ridge which lies at a depth of about 1 km, and it runs parallel to the meridians 137°E and 43°W [*Johnson et al.*, 1990]. Lomonosov Ridge is a continental sliver which broke off from the Barents Sea shelf. Between Europe and the Lomonosov Ridge lies the Eurasian Basin. It is divided by Gakkel Ridge, the currently active Arctic segment of the mid-ocean ridge system, into the 3.8 km deep Nansen Basin on the European side and the 4 km deep Amundsen Basin on the Lomonosov Ridge side.

[41] The opening of the Eurasian Basin probably took place entirely in the Cenozoic, but its initiation is not well constrained. Magnetic lineations as old as Anomaly 24 ($\sim$55 Ma) have been identified, but the time of separation of Lomonosov Ridge from the Barents Sea Shelf has been cited as being as old as 80 Ma [*Rowley and Lottes*, 1988]. *Kristoffersen* [1990] assumed that the opening of the Eurasian Basin began in the late Paleocene, between Anomalies 25 and 24, about 58 Ma. *Weber and Sweeney* [1990] gave the age of Lomonosov Ridge as 65–56 Ma. In any case, the Eurasian Basin did not exist during the Early Cretaceous.

[42] In the western Arctic the older Amerasian Basin lies between Lomonosov Ridge, Alaska, and eastern Siberia. It is also divided into two subbasins by the Mendeleev-Alpha Ridge, the two names referring to the segments abutting the Siberian Shelf off Wrangel Island and Ellesmere Island, respectively. The Mendeleev-Alpha Ridge is variously thought to be a fragment of continental crust (now discounted), an extinct spreading center, an extinct island arc subduction zone, or the trace of a hot spot, aseismic ridge,

or oceanic plateau [*Weber and Sweeney*, 1990]. Between the Lomonosov Ridge and Mendeleev-Alpha Ridge lies the relatively narrow wedge-shaped Makarov Basin, which broadens toward Siberia. Between the Mendeleev-Alpha Ridge, North America, and eastern Siberia lies the Canada Basin, largest of the present Arctic Ocean basins [*Grantz et al.*, 1990]. Because of the uncertainties surrounding the nature of Mendeleev-Alpha Ridge, the nature and age of the Makarov Basin are also uncertain. Although magnetic lineations exist, their interpretation is controversial. Estimates for the age of the opening range from 119 Ma (earliest Aptian) to 97 Ma (latest Albian) [*Tailleur and Brosgé*, 1970], 120 Ma (early Aptian) to 80 Ma (early Campanian) [*Sweeney*, 1985], 125 Ma (Barremian) to 80 Ma (early Campanian) [*Lawver and Baggeroer*, 1983], 130 Ma (Hauterivian) to 100 Ma (late Albian) [*Halgedahl and Jarrard*, 1987], 134 Ma (Valanginian) to 90 Ma (Turonian) [*Rowley and Lottes*, 1988], 140 Ma (Berriasian) to final cessation of spreading about 50 Ma (Early Eocene) [*Lane*, 1997], and 150 Ma (Kimmeridgian) to 90 Ma (Turonian) [*Kazmin and Napatov*, 1998].

[43] There are four very different groups of models for the opening of the Canada Basin, most of which also constrain the nature of Mendeleev-Alpha Ridge and the Makarov Basin (see review by *Lawver and Scotese* [1990]. These consist of rotational, translational, and foundered continent models. The rotational models assume that the northern margin of Alaska is a passive margin that rifted away from Canada and the Arctic Islands, rotating about a pole located near the present Mackenzie River delta or elsewhere in northern Canada. The ‘‘windshield wiper’’ rotation parameters of *Rowley and Lottes* [1988] were used by *Hay et al.* [1999] in their global reconstructions. The translational models propose E-W strike slip motion along the Canadian Arctic Islands or N-S translation with the Arctic Alaskan margin as a transform. Another group of models assumes that much of the crust beneath the western Canada Basin is Paleozoic and belongs to the North American plate.

[44] *Lane* [1997] has made a more detailed analysis of the Canada Basin and surrounding region, including information from Russia, and has concluded that the rotational opening hypothesis can be ruled out. He has proposed a more complex history for the region than any of the four models cited above. His model starts with rifting of Chukotka from North America through formation of a basin parallel to the Canadian margin about the time of the Jurassic-Cretaceous boundary ($\sim$142 Ma). As this basin opened, the South Anyui Ocean Gulf closed; its remnants are found in the ‘‘eugeosynclinal’’ sediments and ophiolites of the North and South Anyui and Anadyr Terranes [*Howell et al.*, 1985]. The floor of this Jurassic-Cretaceous basin is now located off the eastern Siberian margin west of the Chukchi Borderland. At about 90 Ma the spreading center jumped back near the Canadian margin, opening the part of the Canada Basin between the North American margin and Northwind Ridge. A final reorientation of the spreading system in the Late Cretaceous added another 200 km strip of ocean crust. The young Canada Basin may (or may not) have been connected to the closing South Anyui Ocean through a deep passage.

[45] The recent *Kazmin and Napatov* [1998] reconstruction is very similar to that of *Lane* [1997], but includes much more information from the surrounding regions. It shows that the South Anyui Ocean Gulf was a polar oceanic basin that was subducted as the Amerasian Basin formed. The chief difference with *Lane* [1997] lies in timing of the opening phases. *Kazmin and Napatov* [1998] show the initiation of spreading in the Amerasian Basin at $\sim$150 Ma (Volgian) and the cessation at $\sim$80 Ma (Campanian).

[46] Figures 1a–1c show three plate tectonic reconstructions of the Arctic region, for 150, 135, and 120 Ma using the blocks and terranes of *Hay et al.* [1999] but following the scheme and timing of *Lane* [1997] and *Kazmin and Napatov* [1998].

[47] In summary, the new plate tectonic configuration for the Late Jurassic-Early Cretaceous is a large continuous continental block complex (North America, Greenland, and Eurasia) surrounding about 80% of a deep Arctic arm of the Pacific, the ‘‘South Anyui Ocean Gulf.’’ The site of the Greenland-Norwegian Seaway was oriented SSW to NNE and extended from 40° to 50°N latitude.

4.2. Paleogeography

[48] Paleogeography is a function of the plate tectonic configuration, sea level, and orogenic activity. The sections we have studied contain sediments deposited in a narrow meridional seaway between Greenland and Norway. The site (presently 89°N, 140°E) on Lomonosov Ridge where piston cores containing fragments of Jurassic-Early Cretaceous sediments have been recovered [*Grantz et al.*, 2001] was located along a direct continuation of the Greenland-Norwegian seaway. The shape and depth of the seaway may have changed during the Late Jurassic and Early Cretaceous [*Kazmin and Napatov*, 1998]. Our reconstruction for 135 Ma is shown in Figure 1d.

[49] There are no exposures of the strata representing the seaway in Norway, so it is not certain where the eastern shore lay. However, there are exposures of late Jurassic and early Cretaceous strata in Greenland: on the northern side of Scorsby Sund and on Traill and Geographical Society Islands [*Surlyk et al.*, 1981]. These indicate that the western shore was not much further to the west.

[50] Many published reconstructions of Cretaceous paleogeography included space for the Vøring Plateau between Greenland and Norway, resulting in a wide meridional seaway [e.g., *Barron et al.*, 1981]. The paleogeographic reconstructions of *Ziegler* [1982, 1988, 1990] show this broad separation of Norway and Greenland. These reconstructions were originally produced at a time when the nature and age of the Vøring Plateau was not known and overlap of such a large feature with Greenland was unacceptable. However, deep sea drilling has shown that Vøring Plateau was formed during the Eocene as the Norwegian-Greenland Sea opened [*Thiede*, 1980]. The paleogeographic reconstructions of *Ziegler* [1982, 1988, 1990] and *Doré* [1991] show this broad separation of Norway and Greenland and a width of 300–450 km for the seaway.

[51] Using the *Hay et al.* [1999] reconstruction, we can speculate that the seaway was 200–300 km wide and almost 2000 km long. These dimensions correspond closely

to those given by *Bjerrum* [1999] for the seaway in the Toarcian. Because all of the sites are on the same (Eurasian) continental block, the relative distances between them have not changed. The paleolatitudes for the sites are shown in Table 3.

[52] The southern end of the seaway is relatively well known. Only a small part of the Atlantic was already open. The central Atlantic was about 1000 km wide, oriented SW to NE, and extended from near the equator to about 25°N. In many respects it was an analog of the modern Mediterranean. *Ziegler* [1988] showed connections between the Greenland-Norwegian Seaway and the central Atlantic through rift grabens between Greenland, Hatton Bank, Rockall Bank, and the European Block, but these are highly speculative. In any case, they are so long and narrow that they would not have provided effective communication between the two bodies of water. This implies that during the Late Jurassic-Early Cretaceous the southern end of the Greenland-Norwegian Seaway was connected to the Tethyan region across central Europe via a shallow island-rich, NE-SW oriented epicontinental sea about 500 km wide [*Kazmin and Napatov*, 1998]. The northwestern part of this epicontinental sea was the classic "Boreal Realm." The Toarcian paleogeographic reconstruction of this region of *Bjerrum* [1999], compiled from many sources, shows many more islands.

[53] The northern end of the seaway is not well known. Valanginian to Barremian coal-bearing nonmarine beds crop out in Franz Josef Land [*Embry*, 1994] and other small islands between Franz Josef Land and Severnaya Zemlya [*Sokolov*, 1990]. *Ziegler*'s [1988] map for the Berriasian-Barremian shows strait between a "Lomonosov High" and Severnaya Zemlya but is unclear as to whether there was a connection to the South Anyui Ocean Gulf; the critical region lies just beyond the northern border of the map. Recently described bedrock cores from 89°N, 140°E on Lomonosov Ridge [*Grantz et al.*, 2001] (LOM in Figure 1d) contain siltstones similar to those of the coal-bearing strata of Franz Josef Land, but they may be of either Jurassic or Early Cretaceous age. On the basis of zircon grains, they identified the source of the siltstone on Lomonosov Ridge as the Kara Sea region. If the siltstones on Lomonosov Ridge are Early Cretaceous and the Kara Sea provenance is correct, there could not have been a marine connection to the South Anyui Ocean between Franz Josef Land and Severnaya Zemlya.

[54] All of these potential problems are solved if we accept the paleogeography of *Kazmin and Napatov* [1998], who show the Greenland-Norwegian Seaway connected to the South Anyui Ocean Gulf via a strait between Novaya Zemlya and the mainland. As discussed above, the South Anyui Ocean Gulf was a deep arm of the large, open Pacific and has since been completely subducted except for the ophiolitic terranes. If this paleogeography is correct, the interocean passage followed a tortuous path over the European continent. It formed a shallow connection between the deep basins of the Tethys at 25°N and the South Anyui Ocean Gulf at 70–90°N, a straight line distance of about 3500 km. With its curving path the passage from Tethys to Arctic was about 5000 km long. The Greenland-Norwegian segment was the narrowest part of this transcontinental seaway. There was, however, another connection between the Arctic and the Tethys during Tithonian-Barremian times: a broad shallow seaway (Timan-Pechora-Moscow-Precaspian Seaway) extending along the west side of the Urals across the Moscow Platform to the southern margin of the continental block in the present Caucasus region [*Kazmin and Napatov*, 1998]. This shallow seaway met the western passage at the strait between Novaya Zemlya and the mainland.

[55] Across the Jurassic-Cretaceous boundary (Tithonian-Berriasian, ~150–140 Ma), global sea level reached a second order low stand [*Haq et al.*, 1988]. This low stand has been documented within the Greenland-Norwegian Seaway [*Surlyk*, 1990]. The sea level decline reflected globally slow seafloor spreading rates (1.8 cm/year, North Atlantic; 1.3 cm/year, off NW Australia) to the Valanginian (1.2 cm/year, North Atlantic; 1.5 cm/year, off NW Australia; 2.5 cm/year, South Atlantic [*Kominz*, 1984]; Table 1). This sea level lowstand resulted in a general restriction of epicontinental seas [*Ziegler*, 1982, 1988, 1990; *Hardenbol et al.*, 1998].

4.3. Sedimentology

4.3.1. Regional Setting

[56] The Tithonian-Berriasian (150–136 Ma) was characterized by widespread deposition of nonmarine sediments (e.g., the "Wealden facies" in southern England, northern France, and northwest Germany). Siliciclastic sedimentation prevailed in the marine areas during this interval. Endemic marine biota (e.g., ammonites) [*Casey*, 1973; *Hoedemaeker*, 1990; *Rawson*, 1994] developed in the Boreal Realm.

[57] The Valanginian was characterized by widespread transgressions resulting in more open oceanic conditions [*Rawson and Riley*, 1982; *Haq et al.*, 1988; *Ziegler*, 1982, 1988, 1990]. Siliciclastic sedimentation prevailed in middle and high latitudes [*Kazmin and Napatov*, 1998], while the Tethys was characterized by carbonate-rich pelagic sedimentation. The nonmarine Wealden basins of the earlier Cretaceous were partly flooded.

[58] The region surrounding the shallow marine Greenland-Norwegian Seaway was characterized by low hinterland relief. Shoreline sands and offshore muds with channel sands were deposited in east Greenland, along the western side of the seaway [*Surlyk et al.*, 1981; *Emery and Uchupi*, 1984]. Fine-grained sediments were deposited in the basins off mid-Norway and in the Barents Sea, while condensed carbonates accumulated on the structural highs. Local hiatuses formed in late Jurassic-earliest Cretaceous time, thought to be due to differential subsidence with local uplift and erosion.

4.3.2. Sediments in the Seaway

[59] The late Jurassic-early Cretaceous sedimentary succession of the eastern margin of the Greenland-Norwegian Seaway consists of Oxfordian-Berriasian dark C_{org}-rich claystones (Spekk Formation) overlain by late Berriasian-early Valanginian red and grey marls (Lange Formation). To the north the trend from siliciclastics to $CaCO_3$-rich sediments is similar. There the dark C_{org}-rich claystones of Oxfordian-late Berriasian age (Hekkingen Formation) are

Table 4. Ratios of the Hierarchy of Orbital Cycles Compared to the Three Different Types of Bedding Cycles Observed in the Cores[a]

Orbital Cycles	E3	E2	E1	O2	O1	P2	P1
Orbital cycle ratios	1	0.3	0.23	0.12	0.09	0.05	0.04
Type A	1	0.31	0.24	0.13	0.1	n.d.	n.d.
Type B	1	0.31	0.23	0.13	n.d.	0.06	0.05
Type C	1	0.31	0.24	0.13	0.1	0.06	0.05

[a]Numbers are normalized to the E3 eccentricity cycle. Cretaceous values for the orbital cycles are after *Berger et al.* [1992]. N.d., not determined.

overlain by marly limestones of early Valanginian-Barremian age (Klippfisk Formation). According to *Ziegler* [1988], the C_{org}-rich claystones are the principal source rocks from the oil and gas accumulations of the mid-Norway Basin [*Heum et al.*, 1986] and the gas fields of the Barents Sea [*Berglund et al.*, 1986].

4.3.2.1. Cyclic Sedimentation

[60] The spectral analysis shows well-defined peaks with a hierarchical pattern of frequencies. Well-developed examples of each cycle type are shown in Figure 3. For Type A and B cycles we show 10 m intervals, each with 1000 color samples, from Site 6814/04-U-02). Type C cycles are shown in a 5 m interval with 500 samples from Site 6307/07-U-02).

[61] The spectrograms show a pattern of significant peaks; most of those having a power greater than 0.2 are identified in Figure 3. The hierarchical relations of these frequency peaks suggest the influence of orbital cycles. According to *Berger et al.* [1992], Cretaceous eccentricity cycles have periods of 413 ka (E3), 123 ka (E2), and 95 ka (E1), obliquity cycles 50.2 ka (O2) and 38.8 ka (O1), and precession cycles 23.3 ka (P2) and 18.5 ka (P1). The shaded areas in Figure 3 represent deviations of ±3.5% from these peaks, representing a 93% confidence interval [*Nebe*, 1999].

[62] During the Mesozoic the most stable and easily detectable cycle in the rock record is the E3 eccentricity cycle [*Berger et al.*, 1992]. We normalized the frequencies of the Cretaceous orbital cycles to the duration of this cycle, resulting in numerical ratios of 1:0.3:0.23:0.12:0.09:0.05:0.04 = E3:E2:E2:O1:O1:P2:P1. Relative durations of the bedding pattern can be derived by normalizing the peaks in the spectral analysis to the longest one, assumed to be E3 (Table 4). Comparison of the ratios of the orbital frequencies with those determined from spectral analysis of the rock record strongly suggests that the frequencies observed in bedding cycles are determined by orbital forcing.

[63] The correlation between orbital cycles and the sedimentary cyclicity seen by spectral analysis is further supported by a comparison between sedimentation rates derived using two different methods. One method of estimating the sedimentation rate is to assume that it is linear between data of the biostratigraphic record calibrated to the timescale of *Hardenbol et al.* [1998]. A second method of estimating sedimentation rate assumes that the peaks on the spectrogram resulting from spectral analysis of the rock record represent astronomical frequencies and specific durations of time. Comparison of the estimates of sedimentation rates based on these two methods shows close correspondence (Table 5).

[64] Most of the significant peaks with a power greater than 0.2 may be related to orbital frequencies (Table 4). However, there are a few significant peaks on the power spectrum that can not be related to orbital cycles (i.e., the nonshaded double peak in Figure 4a). One of these exceptions is the highest peak of the power spectrumoof Type A cycles; it lies in the range of a possibly orbital-driven 70 ka cycle described by *Rose* [1999].

[65] Type A and B cycles reflect changing sedimentation conditions caused by fluctuations of both carbonate productivity and the redox regime. Orbital forcing is evident at both the low- and high-latitudinal sites in the late Jurassic to early Cretaceous Greenland-Norwegian Seaway. All lithologic cycles are dominantly controlled by eccentricity and obliquity, but Type B and C cycles also show the influence of precession.

[66] The transgressive trend from the early Volgian to the Valanginian is reflected in changing patterns of sedimentation. *Surlyk* [1990] described the Volgian-Valanginian section from the western shore of the seaway in east Greenland. In Jameson Land (north side of Scorsby Sund), fossiliferous, glauconitic cross-bedded dune sandstones of the early-middle Volgian part of the Raukelv Formation are overlain by coarse-grained sandstones of middle Volgian-Valanginian age. These upper sandstones form giant cross beds thought to be of sandbank and dune origin. Omission surfaces at the tops of the sandbank and dunes are thought to represent short-term sea level fluctuations from middle Volgian to early Valanginian time. These may correspond to the cycles seen in the Norwegian shelf sections.

[67] The Type C cycles at the base of the section at Site 6307/07-U-02 were described as silt dilution cycles, suggesting relatively near-shore conditions. During this period the depositional environment was characterized by clastic pulses controlled by orbital forcing. The occurrence of fine terrigenous sediment with high organic carbon content suggests deposition in a shallow basin with restricted circulation.

[68] The deposition of the Spekk Formation took place as sea level rose and the shoreline receded. This sea level rise continued through middle to late Volgian time, but restricted circulation still prevailed. Concretionary cycles of Type B may reflect elevated surface productivity and TOC burial in a sulphate reducing environment.

[69] Fully ventilated marine conditions were finally established in the Valanginian, represented by Type A cycles. These hemipelagic bedding cycles of clay-rich nannoplankton ooze show varying degrees of bioturbation, indicating variable oxygen availability with suboxic to dysoxic conditions during deposition of the carbonate-poor interbeds.

Table 5. Comparison of Two Different Estimates of Sedimentation Rates[a]

Cycle Type	Biostratigraphic SR, m/my	Astronomical SR, m/my
Type A (early Valaginian)	3.8 ± 0.8	4.4 ± 0.2
Type B (late Volgian)	19.0 ± 7.6	16.2 ± 0.4
Type C (early Volgian)	6.7 ± 2.5	8.2 ± 0.4

[a]Biostratigraphic SR = sedimentation rate assuming linear rate between biostratigraphic data using the timescale of *Hardenbol et al.* [1998]. Astronomical SR = sedimentation rate based on assumption that spectral analysis peaks correspond to orbital cycle periods of *Berger et al.* [1992].

[70] The observed transgressive trend was accompanied by cyclicity in both nearshore and open environments. On land, the climate cycles caused variations in weathering and runoff, altering the input of clastic sediment to the sea. Pulses in clastic delivery were essentially synchronous with changes in carbonate and organic carbon production in the seaway. Alternating vigorous and sluggish circulation in the seaway influenced the surface productivity and clastic transport. In the marine realm the climate cycles caused changes in circulation, biological productivity, and degree of oxygenation of interior water masses.

4.3.2.2. Inorganic Geochemistry

[71] The data from our inorganic geochemical investigation suggest suboxic deeper water conditions for the southern sites and oxic, shallower water conditions for the northern sites. The lack of bioturbation, the abundance of framboidal pyrites, the enrichment in trace metals, and the low C/S ratios indicate an anoxic depositional environment within the Volgian-Berriasian TOC-rich sequences.

[72] Higher Ti/Al ratios and high Zr values at Site 6814/04-U-02 either indicate a different provenance for the terrigenous-detrital material or a more energetic (shallower) depositional environment. The enrichment of redox-sensitive and stable sulfide-forming trace metals (As, Cr, Cu, Mo, Ni, U, V, and Zn) in TOC-rich layers suggests anoxic conditions at the sediment surface or in the water column. Sedimentation rates must have been low if seawater served as the excess metal source. The metal enrichments in these dark shales of the Greenland-Norwegian Seaway are comparable to those reported from Cenomanian/Turonian Boundary Event (OAE II; Bonarelli Event) black shales [*Brumsack*, 1980]. The high-Zn values at Site 7430/10-U-01 suggest a supplementary source, perhaps due to hydrothermal activity. The lower trace metal contents (except As and Cr) at Site 6814/04-U-02 suggest a water depth shallower than at Site 6307/07-U-02, indicating that it may have been located on an oceanic plateau. The data also suggest that the central part of the Greenland-Norwegian Seaway was characterized by suboxic bottom waters. Shallower water depths or stronger bottom water currents causing winnowing are indicated by elevated concentrations of elements that are typically enriched in heavy minerals (Ti, Zr, and Cr). Water depths increased towards the Barents Sea Shelf (Site 7430/10-U-01). Sediments at this location show the highest metal enrichments, indicating anoxic conditions. Changes in paleoceanographic conditions are reflected in the Mo/Al ratios (Figures 7a–7d). At Site 6307/07-U-02, Mo/Al ratios reach maximum values between 77 and 92 mbsf, indicating suboxic to anoxic conditions in this interval. They are significantly lower at Site 6814/04-U-02, suggesting less severe oxygen depletion. Mo/Al ratios clearly indicate that anoxic conditions must have prevailed at Site 7430/10-U-01, particularly between 49.0 and 51.5 mbsf. This interval was studied at higher resolution (Figure 7d). Paleoenvironmental conditions seem to have changed in parallel with Milankovitch cycles, as discussed above.

4.3.2.3. Organic Geochemistry

[73] Relatively easily degraded marine organic matter is usually well preserved in the early to middle Volgian strata (lower part of the Spekk and Hekkingen Formations). The samples have high TOC and HI values, heavy $\delta^{13}C$, and contain remains of marine algae as determined by maceral analysis [cf. *Caplan and Bustin*, 1998]. Eutrophic conditions probably prevailed during deposition of these lower organic-rich sequences, promoting algal blooms and rapid settling from the euphotic zone to the seafloor without time for oxidation or recycling. Suboxic to anoxic conditions in the sediments and/or bottom waters aided preservation of large amounts of marine organic matter.

[74] The late Volgian and Berriasian strata (upper part of the Spekk and Hekkingen Formations) contain much highly degraded organic matter, probably derived from algae or humic acid, which generates a high background fluorescence. At the two midlatitudinal Sites (6307/07-U-02 and 6814/04-U-02), there is a significant decrease in TOC and HI toward the top of the section (Figures 8 and 9), indicating increased oxygenation of the water column. This reflects the more open oceanic conditions associated with the rising sea level and a less stratified water column due to increased mixing and breakdown of the pycnocline. The highest Cretaceous unit at Site 6418/04-U-02 (early Hauterivian-early Barremian) is characterized by relatively constant high TOC values (2–3 wt %) and low HI (40–60 mg HC/gTOC). This indicates a stable, oxic environment in which all of the marine organic matter was remineralized but where there was a high terrigenous organic input.

[75] At Site 7430/10-U-01, conditions were very different; the Hekkingen Formation contains organic-rich marine sapropels with very high TOC and HI values (Figures 8 and 9). They were formed predominantly from algae, bituminite, and other lipid-rich land-derived organic matter.

[76] The excellent preservation of easily degraded organic matter, the abundance of freshwater algae, sporinites and bituminous fragments from boghead, and cannel coals all argue for deposition in a restricted shallow basin very close to land rather than an upwelling regime [*Arthur et al.*, 1987; *Taylor et al.*, 1998, R. Littke, personal communication, 2000]. Anoxic conditionsmay have prevailed throughout most of the water column [*Calvert and Pedersen*, 1992; J.S. Sinninghe Damsté, personal communication, 2000]. TOC content of the sediments rises to over 35% at 50 mbsf, then drops rapidly. The Mjølnir Impact layer, with shocked quartz and an iridium anomaly, is at 47.6 mbsf [*Dypvik et al.*, 1996]. Above the impact layer, TOC approaches 0%. It is as though extreme anoxic conditions were building up in this area, but the impact altered conditions so that it was subsequently well ventilated. The impact may have changed the local paleogeography, or the tsunamis it produced may have opened the passage to the Arctic more widely, allowing a greater flow through the seaway. The rapid decline in TOC content of the sediments just beneath the impact may reflect winnowing of the organic matter as sediment was resuspended by the impact tsunamis.

[77] Rock-Eval pyrolysis and maceral analysis show that the composition of the organic matter changes from more marine components in the lower Volgian to more terrigenous components in the Valanginian. However, the size of

terrigenous particles decreases upward along with a decrease of fusinites and an increase of sporinites. The fusinites are plant remains affected by wildfires and may indicate a more arid climate during the time of lower sea level. The sporinites are spores and pollen derived from higher land plants and may indicate a more humid temperate climate during the higher stand of sea level. The decreasing amount of terrestrial detritus may also reflect increasing distance from the coast.

4.4. Paleobiogeography

[78] The latest Jurassic-earliest Cretaceous (Tithonian-Valanginian) is marked by a distinctive provincialism of marine biota. In the Northern Hemisphere, marine floras and faunas show a clear differentiation in two different realms, Tethyan and Boreal. The Boreal Realm includes Russia, northern Europe, Greenland, and Alaska; the Tethys includes the areas further south. The paleobiogeographic patterns have been well documented for various groups of marine organisms, in particular, for calcareous nannofossils [*Wagreich*, 1992; *Mutterlose*, 1992; *Mutterlose and Kessels*, 2000; *Street and Bown*, 2000], brachiopods [*Michalik*, 1992], ammonites [*Hoedemaeker*, 1990; *Rawson*, 1994], belemnites [*Doyle*, 1987; *Mutterlose*, 1988], and bivalves [*Dhondt and Dieni*, 1989; *Dhondt*, 1992]. Endemic marine biota are typical for this interval; the restricted epicontinental seas favored in situ evolution.

[79] High-latitude nannofossil assemblages generally have a low diversity and are characterized by an abundance of *Watznaueria barnesae* and *Crucibiscutum salebrosum*. *C. salebrosum* is extremely common in the Greenland-Norwegian Seaway and the Barents Sea. It shows a bipolar distribution during Valanginian-Hauterivian times, occurring in samples from the Arctic [*Gard and Crux*, 1994] (reworked specimens) and the Greenland-Norwegian Seaway [*Mutterlose and Kessels*, 2000] in the Northern Hemisphere and from Exmouth Plateau and Pacific sites that were at about 50°S at 135 Ma (see interactive fossil distributions at http://www.odsn.de).

[80] *Hay* [2000] noted that for most of the Paleogene, there is no evidence for subtropical or polar frontal systems in the ocean of the Southern Hemisphere. The same is true for most of the Cretaceous (see interactive fossil distributions at www.odsn.de). The occurrence of bipolar assemblages of marine plankton is characteristic only for part of the Early Cretaceous and suggests that the climatic regime was different from the "warm equable" climate of the later Cretaceous.

[81] *Gordon* [1970] discussed the distinctive provincialism in the biogeography of late Jurassic foraminifera. Two zonal assemblages can be recognized: a low-latitude Tethyan assemblage and higher-latitude shelf assemblages in the north and south. The boreal assemblage is characterized by endemic taxa (*Evolutinella, Cribrostomoides*, and *Recurvoides*) [e.g., *Dain*, 1972; *Nagy and Basov*, 1998]. Equatorial assemblages contain more calcareous foraminifera (mainly nodosariids). The earliest planktonic foraminifera (*Conoglobigerina* spp.) occur in the Tethyan Bajocian/Bathonian [*Simmons et al.*, 1997]. In the Middle and Late Jurassic these foraminifera are restricted to south-central and eastern Europe.

[82] Endemic evolution of boreal ammonite taxa started in the mid to Late Jurassic and peaked in Berriasian times. Tethyan and Boreal Realms had not a single ammonite taxon in common [*Hoedemaeker*, 1990]. This paleobiogeographic differentiation is reflected in the use of two different stage names being used for the interval covering the Jurassic/Cretaceous boundary interval: in the Tethys the stage names Tithonian and Berriasian are used, while in the Boreal Realm the terms Volgian and Ryazanian are employed. *Hoedemaeker* [1990] thought that the boundary between the Tethyan and Boreal Realms was at about 60°N in the Berriasian and gradually shifted 12–20° southward during the Valanginian, to around 40°–45°N. However, our reconstruction indicates that it was located at about 30°N during most of the Early Cretaceous. Ammonite migrations occurred during the southward expansion of the Boreal Realm during the Valanginian [e.g., *Kemper et al.*, 1981; *Rawson*, 1994]. Tethyan genera have been recorded from northwest Europe and boreal genera from the marginal areas of the West Mediterranean Province.

[83] Belemnites show a similar biogeographic pattern. The suborder Belemnitidae is known only from the Boreal Realm, while the suborder Belemnopseina is, apart from two exceptions, restricted to the Tethys. This isolation is strongest in Berriasian times and diminishes in the Valanginian. Two Tethyan-derived genera of Belemnopseina have been found in the Valanginian of the Boreal Realm. Although there was northward migration of some Tethyan belemnite genera during the Valanginian, no southward migration of boreal taxa is known.

[84] The changing distribution of marine floras and faunas across the Jurassic-Cretaceous boundary can be best explained by two factors. The first is endemic evolution due to paleobiogeographic isolation in Tithonian-Berriasian times. It was the Valanginian sea level rise that enabled marine biota to attain a more cosmopolitan distribution. The second factor is cool polar conditions for the Berriasian-Valanginian, allowing for bipolar floral belts.

[85] Sea level and climate are ultimately linked, and their effects cannot always be separated. Sea level lowstands correspond to endemism; highstands allow increasing exchange and promote more cosmopolitan assemblages. The relationship between sea level rise and increasing cosmopolitanism of marine biota has been described by many authors [e.g., *Hallam*, 1994].

[86] The foraminiferal assemblages are similar throughout the seaway. The C_{org}-rich muds of the Spekk and Hekingen Formations contain almost exclusively arenaceous foraminifera, but no foraminifera have been found in samples with more than 6% C_{org} The occurrence of *Haplophragmoides*, *Recurvoides*, and *Evolutinella* reflect their high tolerance of unfavorable environmental conditions prevailing during the deposition of C_{org}-rich muds. The faunas of the Volgian/Berriasian interval show similarities to assemblages from Spitsbergen and western Siberia. A flood of *Evolutinella* and *Recurvoides* occurs in earliest Cretaceous samples from Site 6307/07-U-02 (off mid-Norway).

[87] As sedimentation changed from dark mudstones to grey carbonate-rich marls the foraminiferal assemblages became more diverse. Arenaceous forms were joined by calcareous foraminifera (mainly *Lenticulina*, *Globulina*, and *Laevidentalina*) in Valanginian to Hauterivian strata. This diversification occurred during the Valanginian sea level rise. These assemblages and morphogroups can be interpreted as indicating open marine, aerobic, bathyal conditions during the Valanginian. The Valanginian/Hauterivian faunas show affinities with those of NW Europe (Germany, England, and the North Sea). The occurrence of Radiolaria at Sites 6307/07-U-02 and 7430/10-U-01 supports the interpretation of open marine conditions.

4.5. Paleoclimate

[88] Up to the 1980s the paleoclimate of the Cretaceous had been viewed as warm and equable. *Frakes* [1979] and *Hallam* [1981, 1985] considered the Cretaceous to be a period of great warmth over the globe. They thought that tropical-subtropical conditions prevailed to at least 45°N and possibly to 70°S. Warm to cool temperate climates extended to the poles. Mean annual temperatures were significantly higher, and latitudinal gradients were only about half those of today. The $\delta^{18}O$ paleotemperature data from the low-latitude oceans [*Douglas and Woodruff*, 1981] indicated that the Early Cretaceous was only 2–4°C cooler than the Cenomanian. On the basis of a northward shift of Eurasian floras through time, *Vakhrameev* [1964, 1991] concluded that there had been global warming from the Early Jurassic to the mid-Cretaceous. In general, these older studies viewed this as a period free of ice caps [*Hallam*, 1985; *Francis and Frakes*, 1993], and cooling was postulated only for Maastrichtian times. Recently, this view has been questioned, and a much more varied climatic history for the Cretaceous has been suggested [e.g., *Kemper*, 1987; *Stoll and Schrag*, 1996; *Weissert and Lini*, 1991; *Mutterlose and Kessels*, 2000]. *Kemper* [1987] proposed ice ages for the Valanginian and Aptian/Albian that lasted from a few thousand to two million years. *Frakes and Francis* [1988], *Frakes et al.* [1992], and *Ditchfield* [1997] postulated at least seasonall6 cold ocean temperatures and limited polar ice caps for the Early Cretaceous. *Podlaha et al.* [1998], who studied the isotope signature of belemnites from northwest Germany and Speeton (northeast England), proposed warm marine paleotemperatures (20°C) for the Berriasian, a decrease to 15°C in Valanginian and coldest paleotemperatures (10°C) in early Hauterivian times. These interpretations have been confirmed by *Price et al.* [2000], who described relatively warm temperatures for the early Valanginian (12–15°C) and cool temperatures for the earliest Hauterivian (<9°C). For parts of the Early Cretaceous (Berriasian, Valanginian), ice house conditions or at least cool climates have been suggested by the discovery of glendonites of the Gennoishi type in the Valanginian of the Sverdrup Basin from Arctic Canada [*Kemper*, 1987], the changing composition of marine floras and faunas [*Kemper*, 1987], and the occurrence of ice-rafted deposits in Siberia, Australia, and Spitsbergen [*Frakes and Francis*, 1988]. *Weissert and Lini* [1991] argued that stable isotopes also suggest icehouse interludes for the late Early Cretaceous. These include isotope studies on belemnites from northwest Germany and Speeton [*Podlaha et al.*, 1998; *Price et al.*, 2000] and on belemnites from the Lower Cretaceous of Svalbard [*Ditchfield*, 1997]. The nannofossil assemblages from offshore mid-Norway and the Barents Sea [*Mutterlose and Kessels*, 2000; this study] also suggest cold conditions. It is now recognized that climatic changes can occur rapidly and persist for only a short time. Thus many climate variations may have been overlooked. In terms of paleoclimate the Early and mid-Cretaceous may be subdivided into three increasingly warmer intervals: (1) the Berriasian-Hauterivian (142–127 Ma), which is best described as a global ice house world with warm interludes that lasted a few hundred thousand years; (2) the Barremian-early Aptian (127–115 Ma) cited by *Hallam et al.* [1991] and *Ruffell and Batten* [1990] as a time of aridity in northwest Europe, resulting in typical clay mineralogical assemblages; and (3) the late Aptian-Turonian (115–89 Ma) regarded as the mid-Cretaceous greenhouse world by many geologists [e.g., *Larson*, 1991a, 1991b] with warm humid climatic conditions.

[89] Recent climate modeling has shown that during the "warm equable" times, the polar regions may have been characterized by low-pressure systems rather than by highs as at present [*Hay et al.*, 2001a]. In the simulations the polar lows are most strongly developed in winter and almost disappear during summer. The effect of this alternation of strong and weak lows is to result in the strong westerly winds of winter giving way to light and variable winds in summer. Today, the subtropical and polar frontal systems in the ocean are induced by the constant westerly winds. Today, these oceanic frontal systems restrict the distribution of calcareous nannoplankton and planktonic foraminifera. The cosmopolitan nature of the calcareous plankton during much of the Cretaceous and Paleogene can be explained by the seasonal alternation between strong and weak westerly winds. The bipolar distribution of calcareous nannoplankton during the Early Cretaceous implies the existence of at least the subtropical oceanic fronts. These, in turn, imply polar highs, suggesting high polar albedo and ice house conditions.

4.6. Paleoceanography

[90] The Arctic region may have played a critical role in the paleoceanography of the Early Cretaceous. If the waters of the South Anyui Ocean were of normal marine salinity for that time (about 40‰) [*Hay et al.*, 1998; *Floegel et al.*, 2000; *Hay et al.*, 2001a, 2001b, 2001c], it was almost certainly a site of deep water formation. At a salinity of 40‰ the increase in density of water through chilling as it approaches the freezing point is much greater than at modern average ocean salinity of 34.7‰. The deep water would have exited the South Anyui Basin into the world ocean via the open passage to the Pacific. The opening Amerasian Basin may have been connected via a narrow deep passage with the South Anyui Gulf or across a shallow sea over the Arctic Alaska-Bering Blocks, in which case it could also have been a site of deep water production. High-latitude sinking and outflow into the

deep Pacific might have forced one-way (northward) flow through the Greenland-Norwegian Seaway, as postulated in circulation simulations for the seaway for the Jurassic [*Bjerrum*, 1999]. However, it is also possible that there was a land bridge separating the South Anyui Gulf from the Amerasian Basin, so that like the present Arctic Basin, it would have had no deep water connection to the world ocean. The Early Cretaceous was a time of orogenic activity along the southern margin of Asia and the western margin of Canada. This would have directed the flow of rivers northward toward the Arctic Basin. Because of the positive freshwater balance in the Arctic, it is likely that the waters over the Barents and Kara Shelves and in the opening Amerasian Basin had a salinity lower than that of the open ocean. This implies two-way flow through the Greenland-Norwegian and perhaps also the Timan-Pechora-Moscow-Precaspian Seaway. The positive fresh water balance would promote southward outflow of less saline surface water and northward inflow of saline water at depth. There is indeed substantial evidence for low-salinity water in the Canada Basin and inflow into the North American Western Interior Seaway in the Late Cretaceous [*Fisher et al.*, 1994; *Fisher and Hay*, 1999]. Throughout the Volgian-Hauterivian the diversity of benthonic foraminifera in the Greenland-Norwegian Seaway is less than in the central North Sea. Endemic Volgian-Berriasian assemblages give way to cosmopolitan faunas in the Hauterivian, reflecting the global sea level rise. The Volgian-Berriasian *Haplophragmoides-Trochammina* assemblages are closely related to faunas from Spitsbergen, the Sverdrup and West Siberian Basins. There is no relation to assemblages from the North Sea and Northwest Germany. Thus the sea level lowstand (Volgian-Berriasian) goes along with a high rate of endemism, suggesting poor communication through the Seaway, while the sea level highstand (Valanginian-Hauterivian) correlates with cosmopolitan taxa and indicates open communication. Warm water taxa, including *Tritaxia pyramidata* and *Textulariopsis bettenstaedti*, appear in the seaway in the late Valanginian and Hauterivian. These become more common in the younger strata, reflecting a sea level rise and a faunal influx as a result of northward flowing warm bottom waters.

[91] It could be argued that the abundance of *C. salebrosum* in the Greenland-Norwegian Seaway during the early Valanginian [*Mutterlose and Kessels*, 2000] could be the result of either restricted conditions (with consequent endemic evolution) or temperature control. Restricted conditions imply significant separation of the Tethyan and Boreal Realm in the Berriasian and Valanginian, with freshening of the polar waters, lesser exchange and mixing of polar and Tethyan waters. These conditions would favor in situ evolution and would also explain the development of endemic taxa of benthic foraminifera. Temperature control implies cool or cold surface water conditions at high latitudes and significant meridional thermal gradients.

[92] The late Valanginian transgression ended the biogeographic isolation of most biota. There was a decrease in the abundance of endemic taxa and a change to cosmopolitan assemblages. However, the persistent high abundance of *C. salebrosum* in the Hauterivian of the Greenland-Norwegian Seaway samples indicates that the high-latitudinal phytoplankton zones continued to exist. The presence of antipodal high-latitude phytoplankton assemblages in the Southern Hemisphere cannot be explained by endemic evolution of these forms in a semirestricted paleo-Barents Sea. Thus it is more likely that the high-latitude phytoplankton reflect a temperature signal, indicating cool to cold temperatures for the Valanginian and earliest Hauterivian. The Early Cretaceous bipolar distribution of *C. salebrosum* is strong evidence that the high-latitude regions were both cooler and that during this time the "Boreal Realm" of the Northern Hemisphere was not a reflection of lower salinities.

5. Conclusions

[93] The late Jurassic-early Cretaceous sequences offshore mid-Norway and in the Barents Sea reflect (1) a sea level rise throughout the Volgian-Hauterivian period, and (2) a climatic shift from warm humid conditions in Volgian times to arid cold climates in the early Hauterivian (see Figure 12). The bedding pattern of the seaway shows the orbital control of climate, reflected in the nature of depositional changes: fluctuations in the clastic influx and variations in carbonate and organic matter production. Eccentricity, precession, and obliquity signals were prominent in the Greenland-Norwegian Seaway. Trace element concentrations in the Volgian-Berriasian sediments suggest that the central part of the Greenland-Norwegian Seaway might have had suboxic bottom water beneath an oxic water column The lower trace metal contents (except As and Cr) at Site 6814/04-U-02 suggest a shallower water depth than to the south or north.

[94] Both marine and terrigenous organic matter are present in the seaway sediments. The Volgian-Berriasian strata have unusually high contents of organic carbon and are the source rocks for petroleum and gas fields in the region. The accumulation of organic carbon is attributed to restricted conditions in the seaway during this time of low sea level. It might be that the Greenland-Norwegian segment was the deepest part of the transcontinental seaway and that it was bounded at both ends by relatively shallow swells. A shallower swell at Site 6814/04-U-02 may have divided the Greenland-Norwegian Seaway into two "restricted basins." The decline in organic matter content of the sediments in the Valanginian-Hauterivian indicate greater ventilation and more active flow through the seaway as the sea level rose.

[95] The same benthic foraminifera are encountered throughout the seaway; endemic arenaceous assemblages in the Volgian-Berriasian give way to more diverse and cosmopolitan Valanginian-Hauterivian communities that include calcareous species. These assemblages also suggest low oxygen content bottom waters during the earlier time, changing to more fully oxygenation conditions later.

[96] The calcareous nannoplankton, particularly *Crucibiscutum salebrosum*, which is rare at low latitudes and abundant in high latitudes, reflect the meridional thermal

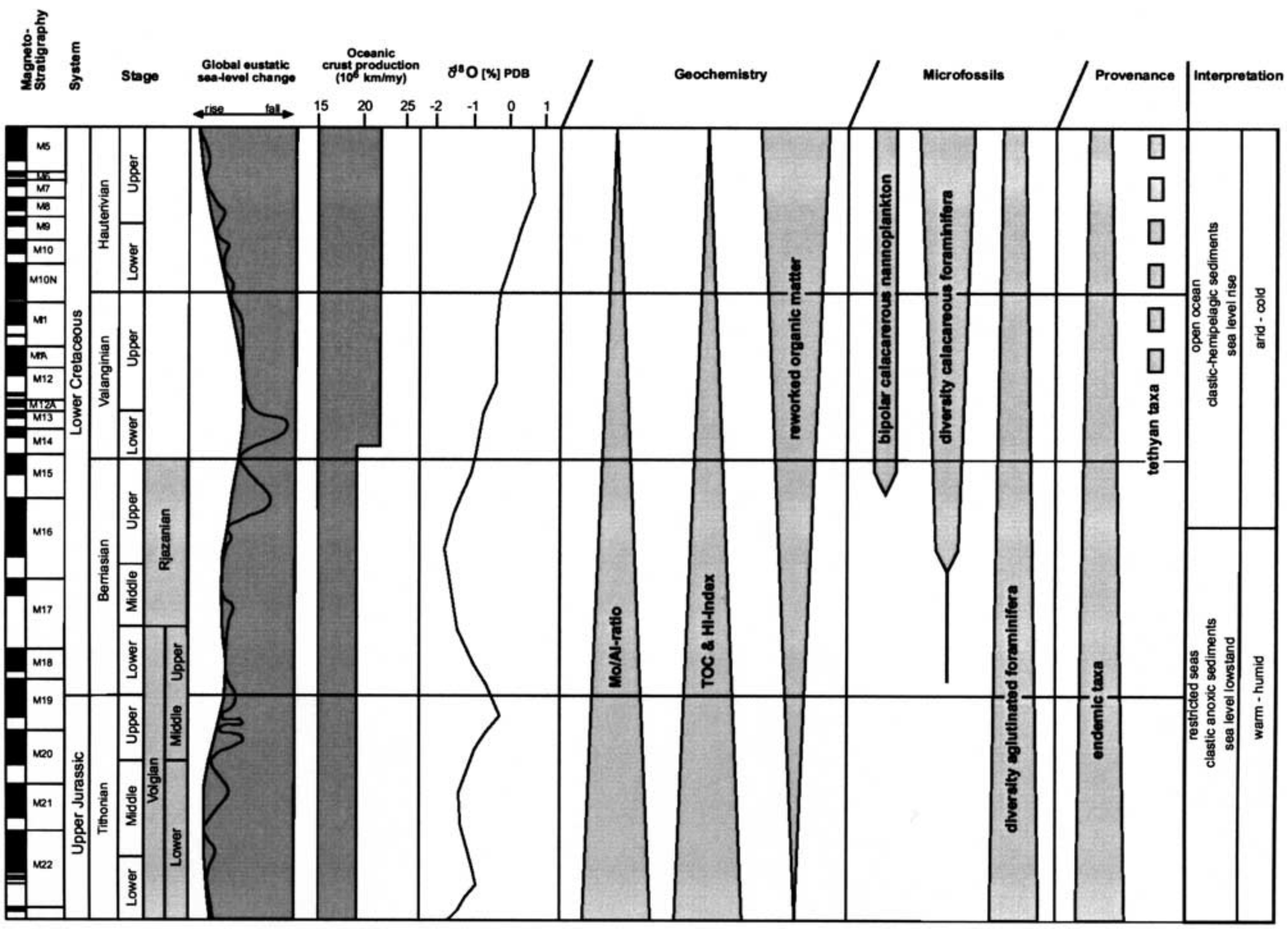

Figure 12. Summary of the results of this study, showing major geochemical and micropaleontological trends. Global eustatic sea level change after *Haq et al.* [1988] and *Gradstein et al.* [1994], oceanic crust production after *Larson* [1991a], and $\delta^{18}O$ ‰ PDB after *Podlaha et al.* [1998].

gradient. They indicate that the Greenland-Norwegian segment of the seaway was north of a frontal zone that acted as a biogeographical barrier. Today, oceanic frontal systems form beneath the maximum of the westerly winds, with the subtropical front at about 45°N and the polar front about 5° further poleward. The paleolatitude of the sites, with 6307/07-U-02 at 43°N, makes it likely that the paleogeographic barrier was a subtropical front developed within the seaway. This implies the existence of stable climatic belts during the early Valanginian and Hauterivian), significant meridional temperature gradients, and moderate "ice house" conditions.

[97] **Acknowledgments.** Financial support by the Deutsche Forschungsgemeinschaft (Br 775/10-1, Ha 2891/3-1, -2, Mu 667/14-1, −2, Ri 525/11-1, Ste 412/13-1) is gratefully acknowledged. SINTEF Petroleum Research (Trondheim) kindly supplied the samples and gave access to unpublished reports. Atle Mørk, Ute Mann, Hermann Weiss, and Morten Smelror (Trondheim) made valuable comments and helped improving the manuscript.

References

Århus, N., The transition from deposition of condensed carbonates to dark claystones in the Lower Cretaceous succession of the southwestern Barents Sea, *Nors. Geol. Tidsskr.*, *71*, 259–263, 1991.

Århus, N., T. Bugge, G. Elvebakk, V. Fjerdingstad, T. L. Leith, A. Mørk, H. Rendall, O. Skarbø, and H. M. Weiss, Shallow drilling Elf Aquitaine/Norsk Hydro/Statoil Barents Sea, 50 pp., *IKU Rep.*, Cont. Shelf Inst., Trondheim, Norway, 1987.

Århus, N., S. R. A. Kelly, J. S. H. Collins, and M. R. Sandy, Systematic palaeontology and biostratigraphy of two Early Cretaceous condensed sections from the Barents Sea, *Polar Res.*, *8*, 165–194, 1990.

Arthur, M. A., S. O. Schlanger, and H. C. Jenkyns, The Cenomanian-Turonian Oceanic Anoxic Event, II, Palaeoceanographic controls on organic matter production and preservation, in *Marine Petroleum Source Rocks*, *Geol. Soc. Spec. Publ. 26*, edited by J. Brooks and A. J. Fleet, pp. 401–420, Blackwell Sci., Malden, Mass., 1987.

Barrera, E., and C. Johnson (Eds.), *Evolution of the Cretaceous Ocean-Climate System*, *Geol. Soc. Am. Spec. Pap. 322*, 445 pp., Geol. Soc. Am., Boulder, Colo., 1999.

Barron, E. J., C. G. A. Harrison, J. L. Sloan, and W. W. Hay, Paleogeography, 180 million years ago to the present, *Eclogae Geol. Helv.*, *74*, 443–470, 1981.

Bartenstein, H., and E. Brand, Mikropaläontologische Untersuchungen zur stratigraphie des nordwestdeutschen valendis, *Abh. Senckenb. Natur. Ges.*, *485*, 239–336, 1951.

Berger, A., M. F. Loutre, and J. Laskar, Stability of the astronomical frequencies over the Earth's history for paleoclimate studies, *Science*, *255*, 560–566, 1992.

Berglund, L. T., J. Augustson, R. Faerseth, J. Gielberg, and H. Ramberg-Moe, The evolution of the Hammerfest basin, in *Habitat of Hydrocarbons on the Norwegian Continental Shelf*, edited by A. M. Spencer, pp. 319–338, Graham and Trotman, Norwell, Mass., 1986.

Bjerrum, C. J., Numerical paleoceanography of a Jurassic narrow meridional seaway: Transcontinental currents and global ocean feedbacks, Ph.D. dissertation, 144 pp., Univ. of Copenhagen, Denmark, 1999.

Bown, P. R., (Ed.), *Calcareous Nannofossil Biostratigraphy*, 314 pp., Chapman and Hall, New York, 1998.

Brumsack, H.-J., Geochemistry of Cretaceous black shales from the Atlantic Ocean, *Chem. Geol.*, *31*, 1–25, 1980.

Bugge, T., et al., Shallow Drilling Barents Sea 1988, *IKU Rep.*, 309 pp., Cont. Shelf Inst., Trondheim, Norway, 1989.

Caplan, M. L., and R. M. Bustin, Paleoceanographic controls on geochemical characteristics of organic-rich Exshaw mudrocks: Role of enhanced primary production, *Org. Geochem.*, *30*, 161–188, 1998.

Casey, R., The ammonite succession at the Jurassic-Cretaceous boundary in eastern England, in *The Boreal Lower Cretaceous*, edited by R. Casey and P. F. Rawson, pp. 193–266, Seel House, Liverpool, UK, 1973.

Churkin, M., Jr., Fold belts of Alaska and Siberia and drift between North America and Asia, in *Proceedings of the Geological Seminar on the North Slope of Alaska*, edited by W. L. Adkison and W. Brosgé, pp. G1–G17, Am. Assoc. Petrol. Geol. Pac. Sect., Bakersfield, Calif., 1970.

Churkin, M. G. R., and J. H. Trexler Jr., Circum-Arctic plate accretion: Isolating part of the Pacific plate to form the nucleus of the Arctic Basin, *Earth Planet. Sci. Lett.*, *49*, 356–362, 1980.

Dain, L. G., (Ed), Foraminifera of the Upper Jurassic deposits of western Siberia (in Russia), *Trudy Vses. Neft. Nauchno-Issled. Geologorazved. Inst. Tekh. Bezop.*, *317*, 273 pp. (In Russian), 1972.

de Graciansky, P. C., E. Brosse, G. Deroo, J.-P. Herbin, L. Montadert, C. Müller, J. Sigal, and A. Schaaf, Organic-rich sediments and palaeoenvironmental reconstructions of the Cretaceous North Atlantic, in *Marine Petroleum Source Rocks*, *Geol. Soc. Spec. Publ. 26*, edited by J. Brooks and A. J. Fleet, pp. 317–344, Blackwell Sci., Norwell, Mass., 1987.

Dercourt, J., L. P. Zonenshain, and L. Ricou, Geological evolution of the Tethys belt from the Atlantic to the Pamirs since the Lias, *Tectonophysics*, *123*, 241–315, 1986.

Dercourt, J., L. E. Ricou, and B. Vrielynck (Eds.), *Atlas Tethys Paleoenvironmental Maps*, 307 pp., Gauthier-Villars, Paris, 1992.

Dhondt, A. V., Palaeogeographic distriubtion of Cretaceous Tethyan non-rudist bivalves, in *New Aspects on Tethyan Cretaceous Fossil Assemblages*, *Schriften. Erdwiss. Kom. Ser.*, vol. 9, edited by H. A. Kollmann and H. Zapfe, pp. 75–94, Springer-Verlag, New York, 1992.

Dhondt, A. V., and I. Dieni, Early Cretaceous bivalves of eastern Sardinia, *Mem. Sci. Geol.*, *40*, 1–97, 1989.

Ditchfield, P. W., High northern palaeolatitude Jurassic-Cretaceous palaeotemperature variation: New data from Kong Karls Land, Svalbard, *Palaeogeogr. Palaeoclimatol. Palaeoecol.*, *130*, 163–175, 1997.

Doré, A. G., The structural foundation and evolution of Mesozoic seaways between Europe and the Arctic, *Palaeogeogr. Palaeoclimatol. Palaeoecol.*, *87*, 441–492, 1991.

Douglas, R. G., and F. Woodruff, Deep sea benthic foraminifera, in *The Sea*, vol. 7, *The Oceanic Lithosphere*, edited by C. Emiliani, pp. 1233–1327, Wiley-Interscience, New York, 1981.

Doyle, P., Lower Jurassic-Lower Cetaceous belemnite biogeography and the development of the Mesozoic Boreal Realm, *Palaeogeogr. Palaeoclimatol. Palaeoecol.*, *61*, 237–254, 1987.

Dypvik, H., S. T. Gudlaugsson, F. Tsikalas, M. Attrep Jr., R. E. Ferrell Jr., D. H. Krinsley, A. Mørk, J. I. Faleide, and J. Nagy, Mjølnir structure: An impact crater in the Barents Sea, *Geology*, *24*, 779–782, 1996.

Einsele, G., *Sedimentary Basins—Evolution, Facies and Sediment Budget*, 2nd ed., 792 pp., Springer-Verlag, New York, 2000.

Embry, A. F., Mesozoic stratigraphy of Franz Josef Land Archipelago, Arctic Russia—A literature review, in *1992 Proceedings, International Conference on Arctic Margins, Anchorage, Alaska, September, 1992*, *OCS Study MMS 94-0040*, edited by D. K. Thurston and K. Fujita, pp. 15–22, U.S. Miner. Manage. Serv., Anchorage, Alaska, 1994.

Emery, K. O., and E. Uchupi, *The Geology of the Atlantic Ocean*, 1050 pp., Springer-Verlag, New York, 1984.

Engleman, E. E., L. L. Jackson, and D. R. Norton, Determination of carbonate carbon in geological materials by coulometric titration, *Chem. Geol.*, *53*, 125–128, 1985.

Espitalié, J., L. Laporte, M. Madec, F. Marquis, P. Leplat, J. Paulet, and A. Boutefeu, Source rock characterization method for petroleum exploration, in *Proceedings of the Ninth Annual Offshore Technology Conference*, vol. 3, pp. 439–443, Okla. Univ., Tulsa, Okla., 1977.

Fisher, C. G., and W. W. Hay, Calcareous nannofossils as indicators of mid-Cretaceous paleofertility along an oceanic front, U.S. Western Interior, in *Evolution of the Cretaceous Ocean/Climate System*, *Geol. Soc. Am. Spec. Pap. 332*, edited by E. Barrera and C. Johnson, pp. 161–180, Geol. Soc. Am., Boulder, Colo., 1999.

Fisher, C. G., W. W. Hay, and D. L. Eicher, Oceanic front in the Greenhorn Sea (late middle through late Cenomanian), *Paleoceanography*, *9*, 879–892, 1994.

Fjerdingstad, V., N. Åhrus, T. Bugge, G. Elvebakk, S. Fanavoll, I. K. Helgesen, T. L. Leith, L. Schou, J. Sættem, and J. O. Vigvan, Shallow Drilling Barents Sea, *IKU Rep.*, 124 pp., Cont. Shelf Inst., Trondheim, Norway, 1985.

Floegel, S., C. N. Wold, and W. W. Hay, Evolution of sediments and ocean salinity, *Abstracts Volume: 31st International Geological Congress: Rio de Janeiro, Brazil, August 6–17, 2000* [CD-ROM], Int. Geol. Conf., Rio de Janeiro, 2000.

Frakes, L. A., *Climates Through Geological Time*, 310 pp., Elsevier Sci., New York, 1979.

Frakes, L. A., and J. E. Francis, A guide to Phanerozoic cold polar climates from high latitude ice-rafting in the Cretaceous, *Nature*, *333*, 547–549, 1988.

Frakes, L. A., J. E. Francis, and J. I. Syktus, *Climate Modes of the Phanerozoic*, 274 pp., Cambridge Univ. Press, New York, 1992.

Francis, J. E., and L. A. Frakes, Cretaceous climates, in *Sedimentology Review 1*, edited by V. P. Wright, pp. 17–30, Blackwell, Malden, Mass., 1993.

Gard, G., and J. A. Crux, Reworked Jurassic-Neogene calcareous nannofossils in the central Arctic, *Mar. Geol.*, *119*, 287–300, 1994.

Gordon, W. A., Biogeography of Jurassic foraminifera, *Bull. Geol. Soc. Am.*, *81*, 1689–1704, 1970.

Gradstein, F. M., F. P. Agterberg, J. G. Ogg, J. Hardenbol, P. van Veen, J. Thierry, and Z. Huang, A Mesozoic timescale, *J. Geophys. Res.*, *99*(B12), 24,051–24,074, 1994.

Grantz, A., S. D. May, P. T. Taylor, and L. A. Lawver, Canada Basin, in *The Arctic Ocean Region*, vol. 50, *The Geology of North America*, edited by A. Grantz et al., pp. 379–402, Geol. Soc. Am., Boulder, Colo., 1990.

Grantz, A., V. L. Pease, D. A. Willard, R. L. Phillips, and D. L. Clark, Bedrock cores from 89°N: Implications for the geologic framework and Neogene paleoceanography of Lomonosov Ridge and a tie to the Barents Shelf, *Geol. Soc. Am. Bull.*, *122*, 1272–1281, 2001.

Gudlaugsson, S. T., Large impact crater in the Barents Sea, *Geology*, *21*, 291–294, 1993.

Halgedahl, S., and R. Jarrard, Paleomagnetism of the Kuparuk River Formation from oriented drill core: Evidence for rotation of the North Slope block, in *Alaskan North Slope Geology*, *Soc. Econ. Paleont. Mineral. Spec. Pub. 50*, edited by I. L. Tailleur and P. Weimer, pp. 581–620, Soc. for Sediment. Geol., Tulsa, Okla., 1987.

Hallam, A., *Facies Interpretation and the Stratigraphic Record*, 291 pp., W. H. Freeman, New York, 1981.

Hallam, A., A review of Mesozoic climates, *J. Geol. Soc. London*, *142*, 433–445, 1985.

Hallam, A., *An Outline of Phanerozoic Biogeography*, *Oxford Biogeogr. Ser. 10*, 246 pp., Oxford Univ. Press, New York, 1994.

Hallam, A., J. A. Grose, and A. H. Ruffell, Palaeoclimatic significance of changes in clay mineralogy across the Jurassic-Cretaceous boundary in England and France, *Palaeogeogr. Palaeoclimatol. Palaeoecol.*, *81*, 173–187, 1991.

Hansen, J. W., et al., Shallow drilling Nordland VI and VII 1991, *IKU Rep.*, 390 pp., Cont. Shelf Inst., Trondheim, Norway, 1991.

Haq, B. U., J. Hardenbol, and P. R. Vail, Mesozoic and Cenozoic chronostratigraphy and cycles of sea-level change, in *Sea Level Changes: An Integrated Approach*, *Soc. Econ. Petrol. Miner. Spec. Publ. 42*, edited by C. K. Wilgus et al., pp. 71–108, Soc. Econ. Petrol. Miner., Tulsa, Okla., 1988.

Hardenbol, J., J. Thierry, M. B. Farley, T. Jacquin, P. C. de Graciansky, and P. R. Vail, Mesozoic and Cenozoic sequence chronostratigraphic framework of European basins, in *Mesozoic and Cenozoic Sequence Stratigraphy of European Basins*, *Soc. Sediment Geol. Spec. Publ. 60*, edited by P. C. Graciansky et al., pp. 7–13, Soc. for Sediment. Geol., Tulsa, Okla., 1998.

Harrison, C. G., and T. Lindh, A polar wandering curve for North America during the Mesozoic and Cenozoic, *J. Geophys. Res.*, *87*, 1903–1920, 1982.

Hay, W. W., Ocean circulation during the Cenozoic, *Abstracts Volume: 31st International Geological Congress: Rio de Janeiro - Brazil, August 6–17, 2000* [CD-ROM], Int. Geol. Conf., Rio de Janeiro, 2000.

Hay, W. W., C. N. Wold, and R. M. DeConto, The role of salinity in circulation of the Cretaceous Ocean, *Zent. Geol. Paläontol. Teil I, 1996, H. 11/12*, 1445–1454, 1998.

Hay, W. W., et al., Alternative global Cretaceous paleogeography, in *Evolution of the Cretaceous Ocean/Climate System*, *Geol. Soc. Am. Spec. Pap. 332*, edited by E. Barrera and C.

Johnson, pp. 1–47, Geol. Soc. Am., Boulder, Colo., 1999.
Hay, W. W., R. M. DeConto, S. Floegel, and E. Soeding, Absence of subtropical and polar fronts in much of the Late Mesozoic and Paleogene, *EUG XI*, *J. Conf. Abstracts*, *6*(1), 140, 2001a.
Hay, W. W., R. M. DeConto, S. Floegel, and E. Soeding, Low atmospheric pressure at the poles during times of warm equable climate, *Geophys. Res. Abstracts*, *3*, 9199, 2001b.
Hay, W. W., C. N. Wold, E. Söding and S. Flögel, Evolution of sediment fluxes and ocean salinity, in *Geologic Modeling and Simulation: Sedimentary Systems*, edited by D. F. Merriam and J. C. Davis, pp. 153–167, Kluwer Acad., New York, 2001c.
Heinrichs, H., and A. G. Herrmann, *Praktikum der Analytischen Geochemie*, 669 pp., Springer-Verlag, New York, 1990.
Heinrichs, H., H.-J. Brumsack, N. Loftfield, and N. König, Verbessertes Druckaufschlusssystem für biologische und anorganische Materialien, *Z. Planzenernährung Bodenkunde*, *149*, 350–353, 1986.
Heum, O. R., A. Dalland, and K. K. Meisingset, Habitat of hydrocarbons at Haltenbanken (PVT-modelling as a predictive tool in hydrocarbon exploration), in *Habitat of Hydrocarbons on the Norwegian Continental Shelf*, edited by A. M. Spencer, pp. 259–274, Graham and Trotman, Norwell, Mass., 1986.
Hoedemaeker, P. J., The Neocomian boundaries of the Tethyan Realm based on the distribution of ammonites, *Cretaceous Res.*, *11*, 331–342, 1990.
Holbourn, A., and M. A. Kaminski, *Lower Cretaceous Deep-Water Benthic Foraminifera of the Indian Ocean*, *Grzybowski Found. Spec. Publ. 4*, 172 pp., Grzybowski Found., Krakow, 1997.
Horna, F., K.-A. Tröger, and S. Vogt (Eds.), *Fifth International Cretaceous Symposium*, 1513 pp., Zent. für Geol. und Paläontol. Teil I 1996, Heft 11/12, Schweiz. Verl., Stuttgart, Germany, 1998.
Howell, D. G., D. L. Jones, and E. R. Schermer, Tectonostratigraphic terranes of the Circum-Pacific region, in *Tectonostratigraphic Terranes of the Circum-Pacific Region*, edited by D. G. Howell, pp. 3–30, Circum-Pac. Counc. for Energy and Miner. Resour., Houston, Tex., 1985.
Huber, B. T., K. G. MacLeod, and S. L. Wing (Eds.), *Warm Climates in Earth History*, 462 pp., Cambridge Univ. Press, New York, 2000.
Huffmann, E. W. D., Jr., Performance of a new automatic carbon dioxide coulometer, *Microchem. J.*, *22*, 567–573, 1977.
Johnson, G. L., A. Grantz, and J. R. Weber, Bathymetry and physiography, in *The Arctic Ocean Region*, vol. 50, *The Geology of North America*, edited by A. Grantz et al., pp. 63–77, Geol. Soc. Am., Boulder, Colo., 1990.
Jongepier, K., J. C. Rui, and K. Grue, Triassic to Early Cretaceous stratigraphic and structural development of the northeastern Møre Basin margin, off Mid-Norway, *Nor. Geol. Tidssk.*, *76*, 199–214, 1996.
Kazmin, V. G., and L. M. Napatov (Eds.), *The Paleogeographic Atlas of Northern Eurasia*, *Inst. Tecton. Lithospheric Plates*, 28 pp., Russ. Acad. Nat. Sci., Moscow, Russia, 1998.
Kemper, E., Das klima der Kreide-Zeit, *Geol. Jahrb. A*, *96*, 5–185, 1987.
Kemper, E., P. F. Rawson, and J.-P. Thieuloy, Ammonites of Tethyan ancestry in the early Lower Cretaceous of northwest Europe, *Palaeontology*, *24*, 251–311, 1981.
Kollmann, H. A., and H. Zapfe (Eds.), *New Aspects on Tethyan Cretaceous Fossil Assemblages*, *Schriften. Erdwiss. Kom. Ser.*, vol. 9, 240 pp., Springer-Verlag, New York, 1992.
Kominz, M. A., Oceanic ridge volumes and sea-level change—An error analysis, in *Interregional Unconformities and Hydrocarbon Accumulation*, *Am. Assoc. Petrol. Geol. Mem. 36*, edited by J. Schlee and S. Schlee, pp. 109–127, Am. Assoc. Petrol. Geol., Tulsa, Okla., 1984.
Kristoffersen, Y., Eurasia Basin, in *The Arctic Ocean Region*, vol. 50, *The Geology of North America*, edited by A. Grantz et al., pp. 365–378, Geol. Soc. Am., Boulder, Colo., 1990.
Lane, L. S., Canada Basin, Arctic Ocean: Evidence against a rotational origin, *Tectonics*, *16*, 363–387, 1997.
Larson, R. L., Latest pulse of Earth: Evidence for a mid-Cretaceous superplume, *Geology*, *19*, 547–550, 1991a.
Larson, R. L., Geological consequences of superplumes, *Geology*, *19*, 963–966, 1991b.
Lawver, L. A., and A. Baggeroer, A note on the age of the Canada Basin, *J. Alaskan Geol. Soc.*, *2*, 57–66, 1983.
Lawver, L. A., and C. R. Scotese, A review of tectonic models for the evolution of the Canadian Basin, in *The Arctic Ocean Region*, vol. 50, *The Geology of North America*, edited by A. Grantz et al., pp. 593–618, Geol. Soc. Am., Boulder, Colo., 1990.
Leith, T. L., et al., Mesozoic hydrocarbon source-rocks of the Arctic region, in *Arctic Geology and Petroleum Potential*, *Norw. Petrol. Soc. Spec. Publ. 2*, edited by T. O. Vorren et al., pp. 1–25, Elsevier Sci., New York, 1992.
Loeblich, A. R., and H. Tappan, *Foraminiferal Genera and Their Classification*, 847 pp., Van Nostrand Reinhold, New York, 1987.
Lomb, N. R., Least-squares frequency analysis of unequally spaced data, *Astrophys. Space Sci.*, *39*, 447–462, 1976.
Michalik, J., The structure and distribution of the European Cretaceous brachiopod assemblages with emphasis on the Tethyan fauna, in *New Aspects on Tethyan Cretaceous Fossil Assemblages*, *Schriften. Erdwiss. Kom. Ser. 9*, edited by H. A. Kollmann and H. Zapfe, pp. 57–74, Springer-Verlag, New York, 1992.
Mutterlose, J., Migration and evolution patterns in Upper Jurassic and Lower Cretaceous belemnites, in *Second International Cephalopod Symposium: Cephalopods: Present and Past, O. H. Schindewolf Symposium*, edited by J. Wiedmann and J. Kullmann, pp. 525–537, Schweiz. Verl., Stuttgart, Germany, 1988.
Mutterlose, J., Biostratigraphy and palaeobiogeography of Early Cretaceous calcareous nannofossils, *Cretaceous Res.*, *13*, 167–189, 1992.
Mutterlose, J., and K. Kessels, Early Cretaceous calcareous nannofossils from high latitudes: Implications for palaeobiogeography and palaeoclimate, *Palaeogeogr. Palaeoclimatol. Palaeoecol.*, *160*, 347–372, 2000.
Nagy, J., and V. A. Basov, Revised foraminiferal taxa and biostratigraphy of Bathonian to Ryazanian deposits in Spitsbergen, *Micropaleontology*, *44*, 217–255, 1998.
Nebe, D. W., Zyklenuntersuchungen an unterkretazischen sedimenten in NW-Deutschland, Ph.D. dissertation, Ruhr Univ. of Bochum, Bochum, Germany, 1999.
Neumayr, M., Über klimatische zonen während der jura und kreidezeit, *Denkschr. Akad. Wiss. Math. Naturwiss. Kl.*, *57*, 277–310, 1883.
Perch-Nielsen, K., Mesozoic calcareous nannofossils, in *Plankton Stratigraphy*, edited by H. M. Bolli, J. M. Saunders, and K. Perch-Nielsen, pp. 329–426, Cambridge Univ. Press, New York, 1985.
Peters, K. E., Guidelines for evaluating petroleum source rock using programmed pyrolysis, *Am. Assoc. Petrol. Geol. Bull.*, *70*, 318–329, 1986.
Podlaha, O. G., J. Mutterlose, and J. Veizer, Preservation of *18O and *13C in belemnite rostra from the Jurassic/Early Cretaceous successions, *Am. J. Sci.*, *298*, 324–347, 1998.
Port, G., Climatic signals recorded in rock magnetic properties of Pleistocene Mediterranean sediments, Ph.D. thesis, Univ. of Cologne, Cologne, Germany, 2001.
Prakash Babu, C., H.-J. Brumsack, and B. Schnetger, Distribution of organic matter in surface sediments along the eastern Arabian Sea: A revisit, *Mar. Geol.*, *162*, 91–103, 1999.
Price, G. D., A. H. Ruffell, C. E. Jones, R. M. Kalin, and J. Mutterlose, Isotopic evidence for temperature variation during the Early Cretaceous (late Ryazanian-mid Hauterivian), *J. Geol. Soc. London*, *155*, 335–343, 2000.
Rawson, P. F., Sea-level changes and their influence on ammonite biogeography in the European Early Cretaceous, *Palaeopelagos Spec. Pub. 1*, 317–326, 1994.
Rawson, P. F., and L. A. Riley, Latest Jurassic-Early Cretaceous events and the "late Cimmerian unconformity" in North Sea area, *Am. Assoc. Petrol. Geol. Bull.*, *66*, 2628–2648, 1982.
Rose, T., High resolution paleo and rock magnetic studies of the cores Kirchrode I and II (Albian, North-West-German Basin), Ph.D. thesis, Univ. of Cologne, Cologne, Germany, 1999.
Rowley, D. B., and A. L. Lottes, Plate-kinematic reconstructions of the North Atlantic and Arctic: Late Jurassic to present, *Tectonophysics*, *155*, 73–120, 1988.
Ruffell, A., and D. Batten, The Barremian-Aptian arid phase in northern Europe, *Palaeogeogr. Palaeoclimatol. Palaeoecol.*, *80*, 197–212, 1990.
Savrda, C. E., and D. J. Bottjer, Trace fossil model for reconstructing oxygenation histories of ancient marine bottom waters: Application to Upper Cretaceous Niobrara Formation, Colorado, *Palaeogeogr. Palaeoclimatol. Palaeoecol.*, *74*, 49–74, 1989.
Scargle, J. D., Studies in astronomical time series analysis—Statistical aspects of spectral analysis of unevenly spaced data, *Astrophys. J.*, *263*, 835–853, 1982.
Simmons, M. D., M. K. BouDagher-Fadel, F. T. Banner, and J. E. Whittaker, The Jurassic Favusellacea, the earliest Globigerinina, in *The Early Evolutionary History of Planktonic Foraminifera*, edited by M. K. BouDagher-Fadel et al., pp. 17–56, Chapman and Hall, New York, 1997.
Skarbø, O., et al., Shallow drilling off Møre-Trøndelag 1988, *IKU Rep.*, 283 pp., Cont. Shelf Inst., Trondheim, Norway, 1988.
Smelror, M., Jurassic stratigraphy of the western Barents Sea region: A review, *GEOBIOS, M.S. 17*, 441–451, 1994.
Smelror, M., T. Jacobsen, L. Rise, O. Skarbø, J. D. Verdenius, and J. O. Vigran, Jurassic to Cretaceous stratigraphy of shallow cores on the Møre Basin Margin, Mid-Norway, *Nor. Geol. Tidssk.*, *74*, 89–107, 1994.
Smelror, M., A. Mørk, E. Monteil, D. Rutledge, and H. Leereveld, The Klippfisk Formation—A new lithostratigraphic unit of Lower Cretac-

eous platform carbonates on the Western Barents Shelf, *Polar Res.*, *17*, 181–202, 1998.

Smelror, M., M. B. E. Mork, H. M. Weiss, and H. Loseth, Middle Jurassic-Lower Cretaceous transgressive-regressive sequences and facies distribution off northern Nordland and Troms, Norway, in *Sedimentary Environments Offshore Norway-Palaeozoic to Recent*, *Spec. Publ.*, vol. 10, edited by O. J. Martinsen and T. Dreyer, pp. 211–232, Elsevier Sci., New York, 2001a.

Smelror, M., H. Dypvik, and A. Mork, Phytoplankton blooms in the Jurassic-Cretaceous boundary beds of the Barents Sea possibly induced by the Mjølnir Impact, in *Geological and Biological Effects of Impact Events*, edited by E. Buffetaut and C. Koeberl, pp. 69–81, Springer-Verlag, New York, 2001b.

Sokolov, R. I., *Geologic Map of Russia and Adjacent Countries (1:5,000,000)*, All Union Res. Geol. Inst., Leningrad, 1990.

Stampfli, G., G. Borel, W. Cavazza, J. Mosar, and P. A. Ziegler, *The Paleotectonic Atlas of the PeriTethyan Domain* [CD-ROM] Eur. Geophys. Soc., Lindau, Germany, 2001.

Stoll, H. M., and D. P. Schrag, Evidence for glacial control of rapid sea-level changes in the Early Cretaceous, *Science*, *272*, 1771–1774, 1996.

Street, C., and P. R. Bown, Palaeobiogeography of Early Cretaceous (Berriasian-Barremian) calcareous nannoplankton, *Mar. Micropaleontol.*, *39*, 265–291, 2000.

Surlyk, F., A Jurassic sea-level curve for East Greenland, *Palaeogeogr. Palaeoclimatol. Palaeoecol.*, *74*, 71–85, 1990.

Surlyk, F., L. B. Clemmensen, and H. C. Larsen, Post Paleozoic evolution of the east Greenland continental margin, in *Geology of the North Atlantic Borderlands*, *Can. Soc. Petrol. Geol. Mem. 7*, edited by J. W. Kerr and A. J. Fergusson, pp. 611–645, Can. Soc. Petrol. Geol., Calgary, 1981.

Sweeney, J. F., Comments about the age of the Canada Basin, *Tectonophysics*, *114*, 1–10, 1985.

Tailleur, I. L., and W. P. Brosgé, Tectonic history of northern Alaska, in *Proceedings of the Geological Seminar on the North Slope of Alaska*, edited by W. L. Adkinson and W. P. Brosgé, pp. E1–E19, Am. Assoc. Petrol. Geol., Pac. Sect., Bakersfield, Calif., 1970.

Taylor, G. H., M. Teichmüller, A. Davis, C. F. K. Diessel, R. Littke, and P. Robert, *Organic Petrology, A New Handbook Incorporating Some Revised Parts of Stach's Textbook of Coal Petrology*, 704 pp., Gebrüder Bornträger, Berlin, 1998.

Thiede, J., Paleo-oceanography, margin stratigraphy, and paleophysiography of the Tertiary North Atlantic and Norwegian-Greenland Seas, *Philos. Trans. R. Soc., London, Ser. A*, *294*, 177–185, 1980.

Tissot, B. P., and D. H. Welte, *Petroleum Formation and Occurrence*, 699 pp., Springer-Verlag, New York, 1984.

Vakhrameev, V. A., *Jurassic and Early Cretaceous Floras of Eurasia and the Paleofloristic Provinces of This Period* (in Russian), *Trans. Geol. Inst. Moscow*, vol. 102, 263 pp., Geol. Inst., Moscow, 1964.

Vakhrameev, V. A., *Jurassic and Cretaceous Floras and Climates of the Earth*, 318 pp., Cambridge Univ. Press, New York, 1991.

Wagreich, M., A review of low-latitude "Tethyan" calcareous nannopankton assemblages of the Cretaceous, in *New Aspects on Tethyan Cretaceous Fossil Assemblages*, *Schriften. Erdwiss. Kom. Ser. 9*, edited by H. A. Kollmann and H. Zapfe, pp. 45–55, Springer-Verlag, New York, 1992.

Weber, J. R., and J. F. Sweeney, Ridges and basins in the central Arctic Ocean, in *The Arctic Ocean Region*, vol. 50, *The Geology of North America*, edited by A. Grantz et al., pp. 305–336, Geol. Soc. Am., Boulder, Colo., 1990.

Weissert, H., and A. Lini, Ice age interludes during the time of Cretaceous greenhouse climate?, in *Controversies in Modern Geology*, edited by D. W. Mueller, J. A. McKenzie, and H. Weissert, pp. 173–191, Academic, San Diego, Calif., 1991.

Wold, C. N., Paleobathymetric reconstruction on a gridded database: The northern North Atlantic and southern Greenland-Iceland-Norwegian Sea, in *Sedimentation and Paleoceanography of the North Atlantic Region*, *Geol. Soc. London Spec. Publ. 90*, edited by R. A. Scrutton et al., pp. 271–302, Blackwell Sci., Norwell, Mass., 1995.

Ziegler, P. A., *Geological Atlas of Western and Central Europe*, 239 pp., Elsevier Sci., New York, 1982.

Ziegler, P. A., *Evolution of the Arctic-North Atlantic and the Western Tethys*, *Am. Assoc. Petrol. Geol. Mem. 43*, 198 pp., Shell Int. Petrol. Maatschapij, The Hague, 1988.

Ziegler, P. A., *Geological Atlas of Western and Central Europe*, 239 pp., Elsevier Sci., New York, 1990.

H. Brumsack and M. Lipinski, Institut für Chemie und Biologie des Meeres (ICBM), Universität Oldenburg, P O Box 2503, D-26111 Oldenburg, Germany. (h.brumsack@geo.icbm.uni-oldenburg.de; m.lipinski@icbm.de)

S. Flögel, W. Hay, and E. Söding, GEOMAR, Forschungszentrum für Marine Geowissenschaften, Wischhofstrasse 1-3, D-24148, Kiel, Germany. (sfloegel@geomar.de; esoeding@geomar.de)

C. Klein and J. Mutterlose, Institut für Geologie, Mineralogie und Geophysik, Ruhr Universität Bochum, Universitätstrasse 150, D-44801 Bochum, Germany. (christian.klein@ruhr-uni-bochum.de; joerg.mutterlose@ruhr-uni-bochum.de)

U. Langrock and R. Stein, Alfred Wegener Institut fur Polar und Marine Research, Columbusstraße, D-27568 Bremerhaven, Germany. (ulangrock-blume@awi-bremerhaven.de; rstein@awi-bremerhaven.de)

W. Ricken and O. Swientek, Geologisches Institut, Sedimentgeologie, Universität Koln, Zülpicher Str. 49a, D-50674 Köln, Germany. (werner.ricken@uni-koeln.de; oliver.swientek@uni-koeln.de)